Trickle infection and immunity to *Trichuris muris*

Maya Glover[1,3¶], Stefano A.P. Colombo[1,2¶], David J. Thornton[1,2], Richard K. Grencis[1,2*]

[1]Lydia Becker Institute of Immunology and Inflammation, University of Manchester, Manchester, United Kingdom.

[2]Wellcome Centre for Cell Matrix Research, University of Manchester, Manchester, United Kingdom

[3]Leucid Bio Ltd, London, United Kingdom

Email: richard.grencis@manchester.ac.uk (RKG)

¶ Maya Glover and Stefano Colombo are joint first authors

Abstract

The majority of experiments investigating the immune response to gastrointestinal helminth infection use a single bolus infection. However, *in situ* individuals are repeatedly infected with low doses. Therefore, to model natural infection, mice were repeatedly infected (trickle infection) with low doses of *Trichuris muris*. Trickle infection resulted in the slow acquisition of immunity reflected by a gradual increase in worm burden followed by a partial expulsion. Flow cytometry revealed that the CD4+ T cell response shifted from Th1 dominated to Th2 dominated, which coincided with an increase in Type 2 cytokines. The development of resistance following trickle infection was associated with increased worm expulsion effector mechanisms including goblet cell hyperplasia, Muc5ac production and increased epithelial cell turn over. Depletion of CD4+ T cells reversed resistance confirming their importance in protective immunity following trickle infection.

In contrast, depletion of group 2 innate lymphoid cells did not alter protective immunity. *T. muris* trickle infection resulted in a dysbiotic mircrobiota which began to recover alpha diversity following the development of resistance.

These data support trickle infection as a robust and informative model for analysis of immunity to chronic intestinal helminth infection more akin to that observed under natural infection conditions and confirms the importance of CD4+ T cell adaptive immunity in host protection.

Author Summary

Infection with parasitic worms (helminths) is a considerable cause of morbidity in humans. Understanding how we respond to infection is crucial to developing novel therapies. Laboratory models of helminth infection have been a valuable tool in understanding fundamental immune responses to infection. However, typically an individual mouse will be infected with a large, single-dose of the parasite. This is in contrast to the natural scenario in which individuals will receive frequent low level exposures. What is unknown is how repeated infection alters the development of immunity to infection. We have developed a laboratory model to tackle this question. We infected mice with the model helminth *Trichuris muris* on a weekly basis and assessed a range of responses in comparison with a more traditional infection system. We found striking differences in the dynamics of the infection, the host immune response, and in changes to host gut microbial populations. Our study shows how resistance to helminth infection can develop over time in response to repeat infection, and provides a model system that better reflects human immunity to this parasite.

Introduction

Gastrointestinal (GI) dwelling nematodes infect approximately 1 billion people worldwide causing significant ill health (1). Prevalence is high in endemic areas although intensity of infection varies

with age, suggesting acquired immunity develops, although sterile immunity is rare and individuals are repeatedly challenged with low numbers of infectious stages throughout their lives (2). Thus, identifying mechanisms of acquired immunity in human populations is extremely challenging, however, data is supportive of acquired immunity driven by Type 2 immunity for at least some if not all the major soil transmitted helminths (STH) *Ascaris lumbricoides*, *Necator americanus*, *Ancylostoma duodenale* and *Trichuris trichiura* (3). Despite this, it appears to be only partial at best and takes considerable time to develop (2,4).

Animal models of intestinal nematode infection have been widely used to help define mechanisms of immunity to these types of pathogen (5). Typically rodents are given a single, and sometimes a second, infection composed of an unnaturally large dose of infectious stages. This approach has been extremely informative and established that such a robust parasite challenge stimulates the host to generate host protective responses, dominated by Type 2 immunity. A clear role for CD4+ Th2 cells is well documented but in addition, recent data indicates that innate immunity plays a major role in host protection through tuft cell induced Type 2 innate lymphoid cell (ILC2) production of IL-13 (6–8). Whilst single bolus infections in the laboratory have been central to defining paradigms of resistance and susceptibility, one major discrepancy between these models and natural infection in man, and indeed rodents, is that individuals are infected repeatedly with low dose infections throughout their lifetime and STH are chronic, non-resolving infections. Studies of repeated low dose nematode infections of rodents are indeed rare (9,10).

The mouse whipworm, *Trichuris muris,* is uniquely placed as a model of the human STH *Trichuris trichiura*, in that it exists as a natural chronic infection of wild rodents. The antigenic cross-reactivity of the two species, similar morphology and same niche of intestinal infection justifies *T. muris* as a suitable parasite to model human infection and has been consolidated by the recent description of the *T. trichiura* and *T. muris* genomes (11,12). Moreover, the immune responses required for resistance and susceptibility to *T. muris* are well established and influenced by both

infective dose and strain of laboratory mouse. C57BL/6 mice that receive a single high dose infection develop resistance, dependent on CD4+ Th2 cells (13) and IL-13 production (14). IL-13 induces a number of effector mechanisms that mediate worm expulsion including accelerated epithelial cell turnover (14–16). *Trichuris* embed in the epithelium of the caecum and with increased epithelial cell turnover the worm is physically carried out of the epithelium into the lumen and expelled. In resistant mice, IL-13 also induces goblet cell hyperplasia and elevated Muc2 and Muc5ac mucins increase during resistance, with deficiency of these mucins causing susceptibility to infection (17).

C57BL/6 mice that receive a single low dose infection of *T. muris* are, in contrast, susceptible and develop a chronic infection associated with CD4+ Th1 cells, IFN-γ production (18) and subsequent regulation via IL-10 (19,20). Chronic low level *Trichuris* infection is associated with a dysbiosis of the intestinal microbiota with a reduction in microbial diversity (21,22) that has a survival benefit for the parasite (23).

Here, we have established a natural trickle infection in the mouse using repeated low doses of eggs to mimic more closely exposure in the field. Following comprehensive immune phenotyping, we now show that repeated low doses of *T. muris* infection results in the slow development of partial resistance with the modification of a Type 1 dominated response to a functionally protective Type 2 immune response. Resistance after this infection regime is dependent on CD4+ T cells and associated with Muc5ac production and an increase in intestinal epithelial cell turnover, confirming their importance even after this multi-infection regime. ILC2s, however, did not appear to play an important role in the development of resistance following *T. muris* trickle infection or indeed after a single high dose infection, which induces complete Type 2 cytokine mediated parasite clearance.

We believe this infection regime presents a powerful approach to further dissect the host/parasite relationship of a major neglected tropic disease, trichuriasis, using a highly relevant mouse model under conditions where the host is challenged by parasite infection in a manner more akin to that seen under natural infecting conditions. Going forward, this provides a more representative platform for analysis of potential vaccine candidates and novel anti-helminthics.

Results

Development of resistance and Type 2 immune responses following *T. muris* trickle infection

To replicate a more natural infection regime of *T. muris,* mice were infected weekly with low doses (20 eggs) for 3, 5, 7 or 9 weeks (S1). Two weeks after the final infection worm burden and immune responses were analyzed. Total worm burden revealed *Trichuris* worm numbers increased through weeks 5 to 9 post infection (p.i.) followed by a significant decrease by week 11 (Fig 1A). Faecal egg counts at week 11 mice followed a similar pattern and suggested a significant reduction in worm burden occurs after week 9 (Fig 1B). When *Trichuris* eggs hatch in the caecum, L1 larvae are released and undergo a series of moults, L2-L4, before developing into adult worms. Larval stages were counted and revealed an absence of early larval stages at week 11 (Fig 1C). Analysis of CD4+ T helper cell subsets from large intestinal lamina propria revealed a shift from a Th1 dominated response during susceptibility at week 9, to a Th2 dominated immune response, associated with resistance at week 11 (Fig 1D). The peak in Th2 cells coincided with an increase capacity to produce IL-13 and no significant change in IFN-γ production (Fig 1E). Analysis of

CD4+ T cell subpopulations from MLNs did not show any significant changes following *T. muris* trickle infection during the period of resistance (S2).

Previous work has demonstrated that antibody responses are not required for resistance to single *T. muris* infections (18,19). Antibody responses specific for *T. muris* adult and larval antigens were analysed following trickle infection. Type 1 IgG2a/c antibody and Type 2 IgG1 antibody steadily increased throughout the complete infection time course (S3). No distinct difference in antibody responses against each larval stage was apparent (excluding responses against L1 antigens which remained low throughout trickle infection). Additionally, total IgE levels did not significantly increase throughout trickle infection (S3).

Goblet cell number and goblet cell size increased consistently throughout the course of the trickle regime peaking at week 11 when resistance had been established (Fig 2A-C). Crypt length, an indicator of gut inflammation, increased during trickle infection (Fig 2D). Sections were stained with HID-AB to visualize the changes in mucin glycosylation in the caecum (Fig 2E). Following low dose *T. muris* infection mucins become sialylated and are more vulnerable to degradation by *T. muris* products (17,24). However, following high dose *T. muris* infection mucins stay sulphated (20). During *T. muris* trickle mucins remained sialylated throughout.

Goblet cells produce a number of protective mucins and secreted proteins during resistance to *T. muris* (17). To determine which goblet cell proteins were correlated with resistance during trickle infection, the expression of a number of goblet cell associated genes was assessed. There was a specific increase in Muc5ac expression at week 11 after trickle infection when resistance developed (Fig 3A). The increase in Muc5ac was confirmed by western blot on secreted mucus. The majority of trickle infected mice showed an increase in secreted Muc5ac (Fig 3B). Muc2 is

also associated with resistance in *T. muris* models of infection (25). Despite no significant increase in gene expression, staining of caecal sections revealed an increase in Muc2 positive cells during the development of resistance in trickle infection (Fig 3C). Relm-β (and to a lesser extent TFF3) have also been associated with resistance in *T. muris* infection (26); despite no increase in TFF3, Relm-β expression significantly increased during the generation of resistance in trickle infection (Fig 3A).

An increase in epithelial cell turnover occurs in resistance of *T. muris* following a high dose infection and hypothesized to physically move the parasite out of its optimal intestinal niche resulting in expulsion (16). To determine whether increased turnover was induced during resistance following trickle infection, mice were injected with BrdU to assess cell turnover (27). A significant increase in epithelial cell turnover was observed during the generation of resistance at week 11 of trickle infection (Fig 4A-B) although, no increase in amphiregulin gene expression was observed (Fig 4C) (27).

Resistance developed following *T. muris* trickle infection is long lasting and protects against subsequent infection

To determine whether the resistance that developed following *T. muris* trickle infection was maintained even in the absence of active infection, trickled mice were challenged following either the natural eventual loss of worms or following anti-helminthic treatment. Faecal egg counts were assessed to determine when all worms had been expelled and the animals were then challenged at week 30. After a single low dose infection, mice were still susceptible to a challenge low dose whereas single high dose infected mice were able to expel a challenge low dose infection. Trickle infected mice were protected against subsequent infection, similar to high dose infected mice (Fig

5A). Mice in which parasites had been removed via anti-helminthic treatment were re-challenged at week 13 with a single low dose of 20 eggs. Compared to naïve control mice, trickle infected mice had significantly lower worm burdens, confirming that trickle infection could generate partial protection to subsequent challenge infections (Fig 5B).

CD4+ T cells are essential for the development of resistance following trickle infection

To determine whether innate or adaptive cells were responsible for the development of resistance following trickle infection, RAG-/- mice were infected with repeated low doses following the week 11 infection regime. Although C57BL/6 mice developed resistance at this time point, RAG-/- mice did not expel worms steadily building up worm numbers, confirming adaptive immune responses were essential for resistance (Fig 6A). To define a role for CD4+ T cells in the development of trickle-induced resistance, C57BL/6 mice were treated with anti-CD4 antibody between week 8 and 11, when we observe resistance developing. Depletion of CD4+ T cells was confirmed by flow cytometry (Fig 6B). This reduction resulted in a significant increase in total worm burden at week 11 which included adult worms and all larval stages (Fig 6 C-D). Furthermore, depletion of CD4+ T cells resulted in a significant reduction in associated effector mechanisms including goblet cell hyperplasia, Muc5ac and Relm-β expression and epithelial cell turnover (Fig 7). There were negligible reductions in the *T. muris* specific antibody response following CD4+ T cell depletion (S4).

Innate lymphoid cells play little role in resistance following *T. muris* trickle infection

ILCs have been shown to play indispensable roles during resistance in multiple model helminth infections including *N. brasiliensis* and *H. polygyrus* (28,29). To determine the role of ILCs during

T. muris trickle infection, ILCs were analysed by flow cytometry. Total intestinal ILC proportions decreased following the development of resistance at week 11 during trickle infection (Fig 8A). Total ILC numbers decreased over the infection period compared to naïve animals and this was reflected by a reduction in ILC2 and ILC3 proportions relative to ILC1s (Fig 8A). Analysis of ILC populations in the MLN showed no changes during the trickle infection regime, including no changes in ILC2 populations (S5). Additionally, previous research has demonstrated that tuft cells proliferate following *N. brasiliensis* and *H. polygyrus* infection and play a key role in inducing expansion of ILC2s by secreting IL-25 (8). During *T. muris* trickle infection there was a small but significant increase tuft cell numbers (identified by dclk1 expression) in the caecum despite a significant decrease in ILC2s at this time point. No change in tuft cell numbers in the small intestine was observed (Fig 8B). To confirm the role of ILC2s during *T. muris* trickle infection, ICOS-T mice that can be specifically depleted for ILC2s by DTx treatment were used (29). Mice were infected repeatedly using the week 11 trickle regime and received DTx or PBS control treatment at week 8-10 when resistance is observed to develop (Fig 9A). DTx treatment resulted in a significant reduction in total ILC2 in the caecum (Fig 9B). This depletion did not alter worm burdens and therefore the development of resistance following *T. muris* trickle infection (Fig 9C). High dose infections (~200 eggs in a single bolus) are a well-established model of Th2-dependent resistance to *T. muris* (30). Using ICOS-T mice, we observe that ILC2 depletion following a single high dose infection did not alter worm expulsion relative to control mice (S6).

Immune responses during trickle infection

A number of studies suggest that individuals naturally infected by helminths have altered susceptibility to atopy and asthma when assessed by skin prick testing to common allergens (31–33). To determine whether *T. muris* trickle infection can alter the allergic response, *T. muris* infected mice were sensitized with the allergen OVA. Local immediate hypersensitivity in the skin

was measured following OVA challenge and revealed that a neither a single low dose or trickle *T. muris* infection altered the local immediate hypersensitivity response as compared to uninfected animals (S7).

In helminth endemic countries it is common to observe that individuals are infected with multiple helminth species include multiple GI nematodes such as whipworm and hookworm (34) and a variety of laboratory co-infection studies have shown that infection by one species of GI nematode can affect the response to another (35–37) although always with single high doses of the respective parasites. In order to investigate the effect of a trickle *T. muris* infection upon another GI nematode infection mice were additionally challenged with a single high dose of *N. brasiliensis* a model of human hookworm infection. However, co-infection following trickle (or indeed a single low dose infection by *T. muris*) did not alter worm expulsion kinetics of *T. muris* or *N. brasiliensis* (S8).

Dysbiosis of the intestinal microbiome begins to resolve following the development of resistance in *T. muris* trickle infection

It has previously been demonstrated that chronic *T. muris* infection following a single low dose infection results in a dysbiotic microbiome (21). Using 16S sequencing we compared changes in the composition of the microbiota between low dose infections and trickle infection (S9). Both low dose and trickle infection induced shifts in the microbiota composition demonstrated by NMDS analysis (Fig 10 A-B). Trickle infection promoted a more significant change in the biota at week 11 compared to the low dose. For low dose infection this change in the microbiota was largely consistent between week 9 and week 11. However, under a trickle infection, at week 11, a partial shift back towards the naïve groups was observed, coinciding with the development of resistance

to infection. To elucidate where these changes were occurring, alpha diversity of the most abundant bacterial phyla were quantified using Shannon indexes. Both infection regimes showed a significant reduction in overall Shannon diversity at week 9 (Fig 10 C-D). However, at week 11 when resistance had developed, population diversity began to recover in trickle infected mice (Fig 11D). This recovery of diversity appeared to predominate in the Bacteriodetes phylum (Fig 10D), and was not seen in low dose infection (Fig 10C). This trend could also be observed at the genus level, where some of the most abundant genera present in the naïve mice at both time points were diminished or could no longer be detected in trickled mice at week 9, but were present at week 11 (Fig 11).

Discussion

Although our knowledge of the immune responses to gastrointestinal nematodes is continuously expanding, the majority of research follows infection after a single high or low dose. However, *in situ* individuals are repeatedly infected with low doses of infection. As human studies are inherently limited and animal models following single infection often show conflicting results when compared to human studies, it is desirable to ensure we are correctly modeling natural infection. Here we functionally characterized the response to infection following a more representative regime by infecting mice repeatedly with low doses, named trickle infection, with the whipworm *T. muris*.

Following trickle infection, we show resistance developed concurrently with intestinal immune responses shifting from CD4+ Th1 cell dominated to a CD4+ Th2 cell dominated response. The development of Type 2 responses coincided with a significant reduction in worm burden including both adult worms and larval stages. Absence of early larval stages suggests that the resistance was targeted/most effective against incoming larval stages. Adult worms, however, persisted until

week 30 shown by continued low faecal egg output. Therefore, only partial resistance was induced, which is similar to that seen in naturally infected individuals with human whipworm (2). Indeed, acquired immunity to most human STHs is slow to develop and incomplete, with 'resistant' individuals in endemic regions harboring low numbers of parasites (2). Previous studies using repeated *T. muris* low dose infection over a much shorter time frame (six infections over a 11 day infection period) suggested host genetics also influenced the capacity to generate resistance, although association between resistance and immune response type was difficult to define (38). Following the present *T. muris* trickle regime the acquisition of resistance was associated with elevated IL-13 production and IL-13-mediated effector mechanisms including goblet cell hyperplasia, Muc5ac production, mucin sulphation, and increased epithelial cell turnover, as seen in previous studies using a single high dose infection to induce resistance (14,16,17,20). Although immunity induced by trickle infection reduced worm numbers significantly it was not able to completely clear infection, as a low level of infection with adult worms persisted. The reasons for this are unclear although may be related to the size and niche occupied by the parasite in combination with ongoing parasite induced immunomodulatory mechanisms (39). For example, adult parasites are extensively embedded within epithelial tunnels, with the anterior of each worm "sewn" through thousands of epithelial cells (40,41) which physically presents a considerable challenge to remove. Previous work has suggested that the IL-13 controlled epithelial escalator was most successful at expelling worms at approximately day 14 post infection when smaller larval stages reside in the lower/mid region of the crypt where epithelial cells move faster (14). Furthermore, following anti-helminthic treatment and challenge infection, trickle infected mice had reduced worm burdens but again were unable to completely expel worms, confirming only partial resistance is induced to even long-term challenge. This would suggest that under conditions of repeated low dose infection such as encountered naturally, complete removal of the parasite burden may be difficult to achieve especially once adult worms are present and given that drug-

298 treatment does not alter immune status significantly. It also predicts that infection would be highly
299 prevalent in the population with most individuals infected by low numbers of worms.
300
301 The data presented here demonstrates a central role for CD4+ T cells in the development of
302 resistance to *T. muris* trickle infection. This is consistent with other models of resistance to
303 *Tirchuris* infection (19,42). Following CD4+ T cell depletion, worm expulsion and associated
304 effector mechanisms were reduced. Robust *T. muris* specific antibody responses were generated
305 during trickle infection, with high levels apparent prior to induction of resistance by week 11.
306 Depletion of CD4+ T cells reduced resistance but had negligible effect upon the antibody
307 response to *T. muris* suggesting little role for antibody in resistance induced by trickle infection.
308 This is in keeping with the data from single high-dose infection studies in *T. muris*, where it is
309 clear that antibody is not required for resistance (19). Also, mice deficient in FcγR are resistant to
310 infection (43), as are mice deficient in Aicda, which are unable to class switch or develop high
311 affinity antibody infection (3i consortium). Interestingly, this is not the case for other models of GI
312 nematode infection such as *H. polygyrus* where antibody does play a role in host resistance
313 particularly during a secondary infection (44). This may reflect the different niches occupied by
314 the parasites underpinning the concept of multiple/redundant Type 2 controlled protective
315 responses against these large multicellular pathogens. This is also evident in the present work
316 regarding the role of ILC2 in host protection. IL-13 is key to resistance to multiple GI nematode
317 infections and ILC2 are a potent source of this cytokine (28,29) with these cells sufficient for
318 resistance to *N. brasiliensis* infection (29). Here we suggest that ILC2s have little/no role in
319 resistance against *T. muris* infection following either a trickle infection or a single high dose
320 infection. A major driver of the ILC2 response following intestinal parasite infection has been
321 identified as the tuft cell, which produces IL-25 promoting ILC2 expansion and IL-13 production
322 (7,8,44). The tuft cell response is muted during *T. muris* infection compared to other systems such

as *N.brasiliensis*, *H. polygyrus* and *T. spiralis* (7,8,45). Previous work has shown that IL-25 null mice are susceptible to a high single dose *T. muris* infection although no increase in IL-25 mRNA expression was found following infection in WT mice. Interestingly, resistance and a Th2 response was recovered in IL-25 null mice when IL-12 was blocked suggesting that resistance did not absolutely require IL-25 (46). The present data supports a poor IL-25 response following *T. muris* infection as evidenced by minimal changes in tuft cell numbers. The difference between *Trichuris* and other model systems studied may be due both the infection regime/dose used and significant differences in life strategies evolved by the different species of parasite. Certainly, most models have used high dose bolus infections to stimulate strong Type 2 immunity including ILC2 responses. A strong induction of ILC2 and as a consequence, a considerable source IL-13, may provide rapid and sufficient induction of appropriate effector mechanisms required to expel the parasites (47). Also, *T. muris* is distinct from other GI model systems in that to progress to patency it induces a Th1 response as part of its strategy to survive whereas even in systems where chronic infection occurs (e.g. *H. polygyrus* infection) it is set against induction and subsequent modulation of a Type2/Th2 response (48).

The intestinal region which *Trichuris* inhabits is also relatively unique when compared to other enteric helminths, with the caecum being its preferred site (16). It is not surprising therefore that *T. muris* can induce an intestinal dysbiosis following chronic infection (21,22) that is dependent upon the presence of worms (21). During trickle infection we now show a dysbiosis in the intestinal microbiome, distinct from single low dose infected mice, that begins to resolve once partial resistance develops. We found that high abundance genera present in naïve mice that were lost or reduced at 9 weeks p.i. in trickled mice were found to return following the observed development of resistance, as well as an overall increase in alpha diversity. It is tempting to speculate that given sufficient time the microbiota would return to a naïve-like phenotype despite the continued presence of *T. muris*. Microbiome studies from humans naturally infected with GI

nematodes including whipworm have been carried out with varied outcomes regarding the influence of helminth infection (49–51). This may be explained in part by cofounding factors including co-infection, diet, age and level of worm burden. However, it has been suggested that *T. trichiura* infection alone is not sufficient to alter the intestinal microbiome (50). Our data supports a more dynamic view of the relationship between the microbiota, and infection and immunity with *Trichuris* species. We suggest that during early recurrent infections, when the host is still susceptible, *Trichuris* alone is capable of driving dysbiosis. However, at the point where a protective immunity is attained, the microbiota will begin to return to a more homeostatic composition characteristic of un-infected individuals.

There is conflicting data as to the influence of chronic helminth/GI nematode infection upon the incidence of allergic responses e.g. skin prick tests in humans (52). With regards to model systems studies using chronic *H. polygyrus* infections have shown that allergic lung responses are muted compared to non-infected animals (53,54) and single low dose chronic infections with *T. muris* also influence lung allergic responsiveness (55). Low dose chronic *T. muris* infection also mutes contact hypersensitivity response to Th1 contact sensitizing agents but not Th2 sensitizing agents (16). Chronic *H. polygyrus* infection modulated responses to both Th1 and Th2 skin sensitizing agents (16). Here, we show that trickle *T. muris* infection does not modulate an immediate (IgE) hypersensitivity response in the skin (nor does a single low dose infection).

It is also common in endemic regions for individuals to be infected by multiple species of GI nematode, including skin penetrating species e.g. hookworm (56–58). In order to assess whether such an infection would influence or be influenced by a *T. muris* trickle infection a single dose of *N. brasiliensis* was superimposed. Neither parasite appeared to be affected in terms of resistance status at least with regards to the timing and challenge regime used here.

375 Overall, the present work demonstrates that partial Type 2 mediated resistance to whipworm,
376 similar to that seen under natural infection, can be generated under laboratory conditions using
377 repeated low dose infection. Functionally, immunity is dependent upon CD4+ Th2 cells and a role
378 for ILC2s could not be established. This approach will complement and extend those models
379 already used for study of immunity to GI nematodes and importantly highlight key differences
380 allowing a more rationale comparison to the field situation.
381

382 **Materials and Methods**

383 **Animals**

384

385 C57BL/6, RAG-/- and iCOS-T (kindly provided by Dr A N McKenzie),(29) mice were maintained
386 in individually ventilated cages in the University of Manchester animal facility in accordance with
387 Home office regulations (1986). Mice were housed for at least 7 days prior to experimentation
388 and were 6-8 weeks old males.

389 **Ethics Statement**

390 Experiments were performed on licence number P043A3082 under the regulation of the Home
391 Office Scientific Procedures Act (1986), and were approved by the University of Manchester
392 Animal Welfare and Ethical Review Body.

393 **Parasitological techniques**

394

395 Mice were infected with *Trichuris muris* embryonated eggs weekly for 3, 5 or 9 weeks. Mice
396 received 20 eggs in 200µl of dH_20 by oral gavage. Two weeks following the final infection, worm
397 burdens and immune responses were analysed. Caeca were collected from infected mice and

parasites sorted into L2, L3, L4 larval stages and adult worms for counting. Faecal egg output was analysed by suspending stool pellets in saturated NaCl and counting in a McMaster Chamber, eggs per g of faeces was calculated.

Mice were infected with 500 *Nippostrongylus brasiliensis* stage 3 larvae (L3) by subcutaneous injection. To determine worm burden of *N. brasiliensis* the lungs and small intestine of infected mice were collected at autopsy. The lungs were placed onto gauze and chopped into small pieces. The gauze containing lung tissue was suspended in 50ml of PBS and incubated at 37°C for 4 hours to allow parasites to move from the tissue and to be counted. The lung tissue was then digested in 1mg/ml collagenase D (Sigma) 0.5mg/ml Dispase (Sigma) in RPMI 1640 medium and incubated at 37°C on a rotator. Digested lung tissue was centrifuged and re-suspended in PBS and parasites were counted. Small intestine was split longitudinally and place in gauze suspended in PBS. After incubation at 37°C for 4 hours, worms were counted.

Production of *T. muris* Excretory/ Secretory products

To produce *T. muris* excretory/secretory products (E/S) for immunological techniques, the parasite was passaged through SCID mice that are susceptible to infection. SCIDs received a high dose of approximately 400 *T. muris* embryonated eggs and at approximately day 35-42 p.i. the large intestine was collected to produce adult E/S. To produce L4 E/S mice were culled at day 28 p.i. To produce L3 E/S mice were culled at day 20 p.i. Guts were collected and longitudinally split open and washed in warmed 5x penicillin/streptomycin in RMPI 1640 medium. Adult, L4 and L3 worms were carefully pulled from the gut using fine forceps and transferred to a 6 well plate containing 4ml warmed 5x pen/strep in RMPI 1640 medium. Plates were placed into a moist humidity box and incubated for 4 hours a 37°C. Adult worms were then split into 2 wells containing

fresh medium and incubated again in a humidity box at 37°C overnight. Supernatant from 4 hour and 24 hour incubation was collected and centrifuged at 2000g for 15 minutes. *T. muris* eggs from adult worms were resuspended in 40ml deionised water and filtered through a 100µm nylon sieve before transferring to a cell culture flask. To allow embryonation, eggs were stored in darkness for approximately 8 weeks and then stored at 4°C. Susceptible mice were subsequently infected with a high dose infection to determine infectivity of each new batch of eggs.

To produce L2 E/S, SCID mice were infected with a high dose of *T. muris* and at day 14 p.i. guts were collected and placed in 5 x pen/strep in PBS. Guts were cut longitudinally and were washed to remove faecal debris. The guts were cut into small sections and added to 0.9% NaCl in PBS and incubated in a water bath at 37°C for two hours to allow L2 larvae to come free from the epithelium.

L2 larvae were removed from the NaCl and placed into 5 x pen/strep RPMI 1640 medium and incubated overnight at 37°C. The following day the larvae and RPMI 1640 medium was centrifuged at 720g and the E/S was recovered.

To produce L1 E/S, eggs were hatched in 2ml sodium hypochlorite (Fisher chemical) in 4ml H_2O for 2 hours at 37°C. L1 larvae were washed in RPMI 1640 medium, 10% FCS, 100 unit/ml of penicillin, 100µl/ml of streptomycin until media returned to original colour. Larvae were cultured at 37°C for 3 weeks with media being collected and replaced twice a week.

All E/S supernatant was collected and filter sterilised through a 0.2 µm syringe filter (Merck). E/S was concentrated using an Amicon Ultra-15 centrifugal filter unit (Millipore) by spinning at 3000g for 15 minutes at 4°C. E/S was dialysed against PBS using Slide-A-Lyzer Dialysis Cassettes, 3.500 MWCO (Thermo Science) at 4°C. The concentration of E/S was measured using the

Nanodrop 1000 spectrophotometer (Thermo Fisher Science) and aliquoted before storing at -20°C.

CD4+ T cell depletion and treatment of iCOS-T mice with diphtheria toxin for innate lymphoid cell 2 depletion

In vivo depletion of CD4+ T cells was achieved by administration of rat IgG2b anti-mouse CD4 (GK1.5, BioXCell). Control animals were treated with the matched isotype control antibody (LTF-2, BioXCell). Animals were treated 3 times a week for 3 weeks with 200µg antibody in 200µl by intraperitoneal (IP) injection.

ICOS-T mice were treated with diphtheria toxin (DTx, Merck) to induce specific depletion of ILC2s. Mice received 750ng DTX in 200µl by IP injection once a day for 5 days. Control mice received a PBS control injection (20).

CD4+ T cell and innate lymphoid cell quantification by Flow cytometry

Lymph nodes were pressed through a 100µm nylon cell strainer (Fisher Scientific) and cells were pelleted by centrifugation at 400g for 5 minutes. The supernatant was removed and the pelleted MLN cells were resuspended in 1ml of complete RPMI.

The large intestine was opened longitudinally with blunt ended scissors and cut into 0.5cm segments before washing in 2% foetal calf serum (FCS) in Hank's Balanced Salt Solution (HBSS) (Sigma, Life Sciences). To remove epithelial cells, large intestine segments were added to 2mM

Ethylenediaminetetraacetic acid (EDTA)/HBSS and incubated on a rotator for 15 minutes at 37°C. Samples were strained through a metal strainer and were washed in 2% FCS HBSS. Gut segments were incubated in EDTA/HBSS for 30 minutes at 37°C on a rotator. To isolate lamina propria lymphocytes (LPLs), large intestine segments were added to an enzyme cocktail of 0.85mg/ml Collagenase V (Sigma), 1.25mg/ml Collagenase D (Roche), 1mg/ml Dispase (Gibco, Life Technologies) and 30µg/ml DNase (Roche) in 10ml complete RPMI (Sigma, Life Sciences). Samples were incubated on a rotator at 37°C for 45 minutes or until all tissue was digested. Samples were passed through a cell strainer (Fisher Scientific resuspended in complete RPMI.

MLN and large intestine cell suspension were stained with 1µl of Fixable Viability Dye (eBioscience) to identify live cells. Samples were fixed and permeabilised using the Foxp3/Transcription Factor Staining Buffer Set (eBioscience) and blocked for non-specific binding by incubating samples in 50µl Anti-Mouse CD16/CD32 Fc Block (eBioscience). Samples were stained for cell surface and intraceullar markers. Samples were read on a BD LSRFortessa flow cytometer (BD Biosciences) running FACSDiva acquisition and analysed using FlowJo X (Tree Star, Inc).

Cell surface markers: primary antibodies anti-CD11b (CR3a); anti-NK1.1 (PK126); anti-Ly6G (Gr-1); anti-CD11c (N418); anti-CD45R (RA3-6B2); anti-CD19 (1D3); anti-TER-119 (TER-119); anti-CD49b (DX5); anti-F4/80 (BM8); anti-FCεR1 (MAR1); anti-CD4 (RM4-5); anti-CD45 (30-F11); anti-CD127 (A7R34); anti-TCR-beta (H57-597) and anti-CD8a (53-6.7) purchased from eBioscience. Primary anti-CD90.2 (30-H12) and secondary streptavidin PE Dazzel purchased from Biolegend. Intracellular markers: anti-GATA3 (16E10A23); anti-Tbet (ebio4BIO); anti-Roryt

(B2D); anti-FOXP3 (FJK-16s) purchased from ebioscience. Primary antibodies were used at dilutions 1:50-1:800. Secondary antibodies used at 1:1000 dilution.

Quantification of parasite specific IgG1 and IgG2a/c by ELISA Blood was collected from mice at autopsy and serum was isolated. ImmunoGrade plates (BrandTech Scientific, Inc) were coated with 5µg/ml *T. muris* excretory secretory (E/S) product from Adult, L4, L2, L2 or L1 parasites. Plates were washed using a Skatron Scan Washer 500 (Molecular Devices, Norway) 5 times with PBST following each incubation. Plates were blocked with 3% bovine serum albumin (BSA). A double dilution of serum samples was added to plates with a starting dilution of 1:20. Biotinylated rat anti-mouse IgG1/c (1:2000, Biorad) or rat anti-mouse IgG2a (1:1000, BD Pharmigen) was added to plates followed by Streptavidin peroxidase (Sigma). Plates were developed with ABTS (10% 2,2'azino 3-thyl benzthiazoline) and read at 405nm with 490nm reference on a Dynex MRX11 microplate reader (Dynex Technologies).

Histology and immunofluorescence

Caecal tips were collected and fixed in Carnoy's solution. Sections were paraffin embedded and 5µm sections were mounted onto slides for staining. To analysed caecal crypts and goblet cell counts sections were stained with periodic acid Schiff's reagent (PAS) and counterstained with Meyers haematoxylin(Sigma). To analyse mucin sulphation, sections were stained with High- Iron Diamine-Alcian Blue (HID-AB). Images were visualised using an Axioskop upright microscope using the Axiovision software.

To stain for Brdu, muc2 and tuft cells, sections were stained with primary anti-BRDU (BU1/75, BioRad), anti-muc2 antibody, 1:200 dilution (5501, gift from D. Thornton) or anti-Dclk1 antibody,

1:800 dilution (Abcam) at 1:800 dilution). Sections were washed in PBS and incubated in secondary antibody goat anti-rabbit Af488 (Life techologies) for 1 hour at room temperature. Nuclear structures were stained with DAPI. An Olympus BX51 upright microscope was used to visualise staining using MetaVue software.

Intestinal microbiome analysis

Stool samples were collected from mice and DNA was extracted using the QIAamp DNA stool mini kit (Qiagen) according to manufacturer's instructions. To charactarise the gut microbiome the 16S rRNA gene was amplified using 16S primers that target the V3/V4 region. Forward primer: 5'-TCGTCGGCAGCGTCAGATGTGTATAAGAGACAGCCTACGGGNGGCWGCAG-3'. Reverse primer: 5'-GTCTCGTGGGCTCGGAGATGTGTATAAGAGACAGGACTACHVGGGTATCTAATCC-3'. Samples were amplified using the following conditions: 10-50 ng of template DNA, 12.5 µL of 2x KAPA HiFi HotStart ReadyMix, 5 µL each of 1 µM forward and reverse primers in a 25 µL reaction. The cycle parameters are as follows: 95°C 3 min, then 25 cycles of 95°C 30 s; 55 °C 30: 72 °C s: with a final step of 72 °C for 3 min. The 16S amplicons were purified using AMPure XP magnetic bead purification. Samples were indexed using the Nextera XT index kit and then quantified by Illumina Miseq in the Genomic Technologies Core Facility at the University of Manchester. Sequences were trimmed using Trimmomatic then clustered into OTUs with a sequence similarity of 97% and taxonomy was assigned in QIIME (59) using the SILVA132 database. Statistical analysis and non-metric Multidimensional Scaling (NMDS) were performed using the R-package. OTU counts were normalised using the DESeq2 package (60). Shannon diversity, PERMANOVA tests, and rarefaction were performed using the Vegan package. NMDS plots represent Euclidian distances plotted in arbitrary two dimensional space centred on

zero. Stress is a measure of quality of fit of Bray-Curtis dissimilarities where less than 0.2 indicates good fit on two dimensional plots. NMDS and bubble graphs were produced using the ggplot2 package.

Gene expression of gut associated genes

Caecal tips were collected at autopsy and RNA was extracted using the TRIzol method (Invitrogen). cDNA was generating using the GoScript Reverse Transcriptase kit (Promega). Quantitative-PCR was set up using the SensiFAST SYBR Hi-ROX kit (Bioline) on a StepONE system (Applied Biosytems). Genes of interest were normalised against β-actin and expressed as fold change compared to naïve mRNA expression. Muc2: F:5'GTCCAGGGTCTGGATCACA. R:5' CAGATGGCAGTGAGCTGAGC. Muc5ac: F:5' GTGATGCACCCATGATCTATTTTG R:5; ACTCGGAGCTATAACAGGTCATGTC. Relm-β: F:5' GCTCTTCCCTTTCCTTCTCCAA R:5' AACACAGTGTAGGCTTCATGCTGTA. TFF3: F:5' TTATGCTGTTGGTGGTCCTG. R:5' CAGCCACGGTTGTTACACTG. β-actin: F: 5' TCTTGGGTATGGAATGTGGCA R:5'ACAGCACTGTGTTGGCATAGAGGT. TSLP: F:5' AGCAAGCCAGTCTGTCTCGTGAAA R: TGTGCCAATTCCTGAGTACCGTCA Ampliregulin: F:5' TCTGCCATCATCCTCGCAGCTATT R:5' CGGTGTGGCTTGGCAATGATTCAA. Bacterial load: F: 5' TCCTACGGGAGGCAGCAG. R: 5' GGACTACCAGGGTATCTAATCTT.

Mucus extraction and analysis

Mucus was extracted by flushing large intestines with PBS and shaking in 2M urea. Samples were reduced by dithiothreitol (DTT) and run on a 1% agarose gel in TAE buffer. Mucins were transferred onto a nitrocellular membrane, blocked with casein and probed using chicken anti-

mouse Muc5ac antibody (Rockland) followed by an incubation with the goat anti-chicken IgY AF790 (Abcam). The membrane was imaged using the Odyssey CLx Imaging system (Licor) on Image studio software (15).

MLN re-stimulation and cytokine analysis by Cytometric bead assay (CBA)

Mesenteric lymph nodes (MLNs) were isolated at autopsy and cells were restimulated with 50µg/ml *T. muris* adult ES. Cells were incubated for 48 hours at 37°C, 5% CO2. Supernatant from cell cultures were incubated with a capture bead cocktail for cytokines of interest (BD Bioscience), containing one for each cytokine. Detection beads (BD Bioscience), diluted in detection reagent (BD Bioscience) was added to each well and incubated. Plates were washed and resuspended in 70µl wash buffer (BD Bioscience). Cytokines were measured on a MACSQuant Analyser (Miltenyi Biotec) and analysed using the FCAP array software in reference to a standard curve.

Measurement of skin immediate hypersensitivity

Mice were sensitised with 50µg ovalbumin (OVA, Sigma) in 2mg Alum (Thermo Scientific) by I.P. injection. Control mice were injected with PBS in Alum. Mice received one dose a week for 3 weeks. Two weeks after the final injection the anaphylaxis assay was performed.

Mice were anesthetised by 2% isoflurane. Mice were injected subcutaneously with 5µg OVA in 10µl PBS into one ear and 10µl PBS into the other. The ear was stabilised onto a falcon tube to aid injections. After 3 minutes 200µl of 0.5% Evans Blue dye (Sigma) was injected into the tail

vein. After 10 minutes, mice were euthanised and ears were removed and placed into 700µl Formamide (Sigma). The ears were incubated overnight at 63°C to allow dye to leak into the Formamide. 300µl of each sample was transferred into a 96 well plate in duplicate and read on a VersaMax Microplate reader (Molecular Devices) at 620nm.

Statistical analysis

Statistical analysis completed using a one-way ANOVA, followed by post-hoc Tukey's test or an unpaired t-test using GraphPad Prism 7 software.

Acknowledgements

We thank A. McKenzie (LMB) for providing iCOS-T mice; A. Bancroft for help with infection; L. Campbell for help with immediate hypersensitivity experiments; M. Lawson for advice and feedback on microbiota analysis. We also thank the Faculty of Biology, Medicine & Health core facility services at the University of Manchester, including Genomic Technologies, Histology, Flow Cytometry, BSF, and Bioimaging. In particular we thank P. Wang in the Bioinformatics Core Facility for his help in the processing of sequencing data.

References

1. Pullan RL, Smith JL, Jasrasaria R, Brooker SJ. Global numbers of infection and disease burden of soil transmitted helminth infections in 2010. Parasites and Vectors. 2014;7(1):1–19.
2. Cooper PJ. Mucosal immunology of geohelminth infections in humans. Mucosal Immunol. 2009;2(4):288–99.

3. Hotez PJ, Pearce EJ, Jacobson J, Hotez PJ, Brindley PJ, Bethony JM, et al. Helminth infections : the great neglected tropical diseases Find the latest version : Review series Helminth infections : the great neglected tropical diseases. J Clin Invest. 2008;118(4):1311–21.
4. Hotez PJ, Alvarado M, Basanez MG, Bolliger I, Bourne R, Boussinesq M, et al. The Global Burden of Disease Study 2010: Interpretation and Implications for the Neglected Tropical Diseases. PLoS Negl Trop Dis. 2014;8(7).
5. Grencis RK. Immunity to Helminths: Resistance, Regulation, and Susceptibility to Gastrointestinal Nematodes. Annu Rev Immunol. 2015;33(1):201–25.
6. Gerbe F, Sidot E, Smyth DJ, Ohmoto M, Matsumoto I, Dardalhon V, et al. Intestinal epithelial tuft cells initiate type 2 mucosal immunity to helminth parasites. Nature. 2016;529(7585):226–30.
7. Von Moltke J, Ji M, Liang HE, Locksley RM. Tuft-cell-derived IL-25 regulates an intestinal ILC2-epithelial response circuit. Nature. 2016;529(7585):221–5.
8. Lavoie S, Michaud M, Tran S V., Margolskee RF, Gallini CA, Weinstock J V., et al. Tuft cells, taste-chemosensory cells, orchestrate parasite type 2 immunity in the gut. Science (80-). 2016;351(6279):1329–33.
9. Ovington KS. Trickle infections of Nippostrongylus brasiliensis in rats. Z Parasitenkd. 1986;72(6):851–3.
10. Brailsford TJ, Behnke JM. The dynamics of trickle infections with Ancylostoma ceylanicum in inbred hamsters. Parasitology. 1992 Oct;105 (Pt 2):247–53.
11. Roach, T.I.A.; Wakelin, D.; Else, K.J.; Bundy DA. Antigenic cross-reactivity between the human whipworm, Trichuris trichiura, and the mouse trichuroids Trichuris muris and Trichinella spiralis. Parasite Immunol. 1988;10(3):279–91.
12. Foth BJ, Tsai IJ, Reid AJ, Bancroft AJ, Nichol S, Tracey A, et al. Whipworm genome and dual-species transcriptome analyses provide molecular insights into an intimate host-parasite interaction. Nat Genet. 2014;46(7):693–700.
13. Else KJ, Grencis RK. Cellular immune responses to the murine nematode parasite Trichuris muris. I. Differential cytokine production during acute or chronic infection. Immunology. 1991;72(4):508–13.
14. Cliffe LJ, Humphreys NE, Lane TE, Potten CS, Booth C, Grencis RK. Accelerated Intestinal Epithelial Cell Turnover: A New Mechanism of Parasite Expulsion Author(s): Laura J. Cliffe, Neil E. Humphreys, Thomas E. Lane, Chris S. Potten, Cath Booth and Richard K. Grencis Source: Science (80-). 2005;308(5727):1463–5.
15. Bancroft AJ, McKenzie AN, Grencis RK. A critical role for IL-13 in resistance to intestinal nematode infection. J Immunol. 1998;160(7):3453–61.
16. Cliffe LJ, Grencis RK. The Trichuris muris System: a Paradigm of Resistance and Susceptibility to Intestinal Nematode Infection. 2004;57(04):255–307.
17. Hasnain SZ, Evans CM, Roy M, Gallagher AL, Kindrachuk KN, Barron L, et al. Muc5ac: a critical component mediating the rejection of enteric nematodes. J Exp Med. 2011;208(5):893–900.
18. Selby GR, Wakelin D. Transfer of immunity against Trichuris muris in the mouse by serum and cells. Int J Parasitol. 1973;3(6):717–21.
19. Else KJ, Grencis RK. Antibody-independent effector mechanisms in resistance to the intestinal nematode parasite Trichuris muris. Infect Immun. 1996;64(8):2950–

4.
20. Hasnain SZ, Dawson PA, Lourie R, Hutson P, Tong H, Grencis RK, et al. Immune-driven alterations in mucin sulphation is an important mediator of Trichuris muris helminth expulsion. PLoS Pathog. 2017;13(2):1–20.
21. Houlden A, Hayes KS, Bancroft AJ, Worthington JJ, Wang P, Grencis RK, et al. Chronic Trichuris muris infection in C57BL/6 mice causes significant changes in host microbiota and metabolome: Effects reversed by pathogen clearance. PLoS One. 2015;10(5).
22. Holm JB, Sorobetea D, Kiilerich P, Ramayo-Caldas Y, Estellé J, Ma T, et al. Chronic Trichuris muris infection decreases diversity of the intestinal microbiota and concomitantly increases the abundance of lactobacilli. PLoS One. 2015;10(5):1–22.
23. White EC, Houlden A, Bancroft AJ, Goldrick M, Hayes KS, Roberts IS, et al. Manipulation of host and parasite microbiotas: Survival strategies during chronic nematode infection. Sci Adv. 2018;4(3):eaap7399.
24. Hasnain SZ, McGuckin MA, Grencis RK, Thornton DJ. Serine Protease(s) Secreted by the Nematode Trichuris muris Degrade the Mucus Barrier. PLoS Negl Trop Dis. 2012;6(10).
25. Hasnain SZ, Wang H, Ghia JE, Haq N, Deng Y, Velcich A, et al. Mucin Gene Deficiency in Mice Impairs Host Resistance to an Enteric Parasitic Infection. Gastroenterology. 2010;138(5):1763-1771.e5.
26. Artis D, Wang ML, Keilbaugh SA, He W, Brenes M, Swain GP, et al. RELMbeta/FIZZ2 is a goblet cell-specific immune-effector molecule in the gastrointestinal tract. Proc Natl Acad Sci U S A. 2004;101(37):13596–600.
27. Zaiss DM, Yang L, Shah PR, Kobie JJ, Urban JF, Mosmann TR. Amphiregulin, a T H 2 cytokine enhancing resistance to nematodes. Science (80-). 2006;314(5806):1746.
28. Pelly VS, Kannan Y, Coomes SM, Entwistle LJ, Rückerl D, Seddon B, et al. IL-4-producing ILC2s are required for the differentiation of TH2 cells following Heligmosomoides polygyrus infection. Mucosal Immunol. 2016;
29. Oliphant CJ, Hwang YY, Walker JA, Salimi M, Wong SH, Brewer JM, et al. MHCII-mediated dialog between group 2 innate lymphoid cells and CD4 + T cells potentiates type 2 immunity and promotes parasitic helminth expulsion. Immunity. 2014;41(2):283–95.
30. Else KJ, Finkelman FD, Maliszewski CR, Grencis RK. Cytokine-mediated regulation of chronic intestinal helminth infection. J Exp Med. 1994;179(1):347–51.
31. Van Den Biggelaar AHJ, Van Ree R, Rodrigues LC, Lell B, Deelder AM, Kremsner PG, et al. Decreased atopy in children infected with Schistosoma haematobium: A role for parasite-induced interleukin-10. Lancet. 2000;356(9243):1723–7.
32. Chico ME, Vaca MG, Rodriguez A, Cooper PJ. Soil-transmitted helminth parasites and allergy: Observations from Ecuador. Parasite Immunol. 2018;(June 2018):1–11.
33. Mpairwe H, Amoah AS. Parasites and allergy: Observations from Africa. Parasite Immunol. 2018;(July):1–9.

34. Mohammed KA, Khamis IS, Lello J, Viney ME, Knopp S, Utzinger J. The relative contribution of co-infection to focal infection risk in children. Proc R Soc B Biol Sci. 2013;280(1754):20122813–20122813.
35. Behnke JM, Wakelin D, Wilson MM. Trichinella spiralis: Delayed rejection in mice concurrently infected with Nematospiroides dubius. Exp Parasitol. 1978;46(1):121–30.
36. Jenkins SN, Behnke JM. Impairment of primary expulsion of trichuris muris in mice concurrently infected with nematospiroides dubius. Parasitology. 1977;75(1):71–8.
37. Behnke JM, Ali NMH, Jenkins SN. Survival to patency of low level infections with Trichuris muris in mice concurrently infected with Nematospiroides dubius. Ann Trop Med Parasitol. 1984;78(5):509–17.
38. Bancroft AJ, Else KJ, Humphreys NE, Grencis RK. The effect of challenge and trickle Trichuris muris infections on the polarisation of the immune response. Int J Parasitol. 2001;31(14):1627–37.
39. Bancroft AJ, Levy CW, Jowitt TA, Hayes KS, Thompson S, Mckenzie EA, et al. The major secreted protein of the whipworm parasite tethers to matrix and inhibits interleukin-13 function. Nat Commun. 2019;10(1):2344.
40. Lee TDG, Wright KA. The morphology of the attachment and probable feeding site of the nematode Trichuris muris (Schrank, 1788) Hall, 1916. Can J Zool. 1978;56(9):1889–905.
41. Tilney LG, Connelly PS, Guild GM, Vranich KA, Artis D. Adaptation of a nematode parasite to living within the mammalian epithelium. J Exp Zool Part A Comp Exp Biol. 2005;303(11):927–45.
42. Betts J, deSchoolmeester ML, Else KJ. Trichuris muris: CD4+ T cell-mediated protection in reconstituted SCID mice. Parasitology. 2000;121 Pt 6(May):631–7.
43. Betts CJ, Else KJ, Elisa M-. Mast cells are not critical in resistance to Trichuris muris. 1999;(May 1998):45–52.
44. McCoy KD, Stoel M, Stettler R, Merky P, Fink K, Senn BM, et al. Polyclonal and Specific Antibodies Mediate Protective Immunity against Enteric Helminth Infection. Cell Host Microbe. 2008;4(4):362–73.
45. Gerbe F, Legraverend C, Jay P. The intestinal epithelium tuft cells: Specification and function. Cell Mol Life Sci. 2012;69(17):2907–17.
46. Owyang AM, Zaph C, Wilson EH, Guild KJ, McClanahan T, Miller HRP, et al. Interleukin 25 regulates type 2 cytokine-dependent immunity and limits chronic inflammation in the gastrointestinal tract. J Exp Med. 2006;203(4):843–9.
47. Klose CSN, Mahlakõiv T, Moeller JB, Rankin LC, Flamar AL, Kabata H, et al. The neuropeptide neuromedin U stimulates innate lymphoid cells and type 2 inflammation. Nature. 2017;549(7671):282–6.
48. Maizels RM, Smits HH, McSorley HJ. Modulation of Host Immunity by Helminths: The Expanding Repertoire of Parasite Effector Molecules. Immunity. 2018;49(5):801–18.
49. Lee SC, Tang MS, Lim YAL, Choy SH, Kurtz ZD, Cox LM, et al. Helminth Colonization Is Associated with Increased Diversity of the Gut Microbiota. PLoS Negl Trop Dis. 2014;8(5).
50. Cooper P, Walker AW, Reyes J, Chico M, Salter SJ, Vaca M, et al. Patent Human

Infections with the Whipworm, Trichuris trichiura, Are Not Associated with Alterations in the Faecal Microbiota. PLoS One. 2013;8(10).
51. Rosa BA, Supali T, Gankpala L, Djuardi Y, Sartono E, Zhou Y, et al. Differential human gut microbiome assemblages during soil-transmitted helminth infections in Indonesia and Liberia. Microbiome. 2018;6(1):1–19.
52. Alcantara-Neves NM, Veiga R V., Ponte JCM, Da Cunha SS, Simöes SM, Cruz ÁA, et al. Dissociation between skin test reactivity and anti-aeroallergen IgE: Determinants among urban Brazilian children. PLoS One. 2017;12(3):1–13.
53. Wilson MS, Taylor MD, Balic A, Finney CAM, Lamb JR, Maizels RM. Suppression of allergic airway inflammation by helminth-induced regulatory T cells. J Exp Med. 2005;202(9):1199–212.
54. Zaiss MM, Rapin A, Lebon L, Dubey LK, Mosconi I, Sarter K, et al. The Intestinal Microbiota Contributes to the Ability of Helminths to Modulate Allergic Inflammation. Immunity. 2015;43(5):998–1010.
55. Chenery AL, Antignano F, Burrows K, Scheer S, Perona-Wright G, Zaph C. Low-Dose Intestinal Trichuris muris Infection Alters the Lung Immune Microenvironment and Can Suppress Allergic Airway Inflammation. Infect Immun. 2016;84(2):491–501.
56. Kan SP. Soil-transmitted helminthiasis in Selangor, Malaysia. Med J Malaysia. 1982;37(2):180–90.
57. Al-Delaimy AK, Al-Mekhlafi HM, Nasr NA, Sady H, Atroosh WM, Nashiry M, et al. Epidemiology of Intestinal Polyparasitism among Orang Asli School Children in Rural Malaysia. PLoS Negl Trop Dis. 2014;8(8).
58. Raso G, Luginbühl A, Adjoua CA, Tian-Bi NT, Silué KD, Matthys B, et al. Multiple parasite infections and their relationship to self-reported morbidity in a community of rural Côte d'Ivoire. Int J Epidemiol. 2004;33(5):1092–102.
59. Caporaso JG, Kuczynski J, Stombaugh J, Bittinger K, Bushman FD, Costello EK, et al. QIIME allows analysis of high- throughput community sequencing data Intensity normalization improves color calling in SOLiD sequencing. Nat Publ Gr. 2010;7(5):335–6.
60. Love MI, Huber W, Anders S. Moderated estimation of fold change and dispersion for RNA-seq data with DESeq2. Genome Biol. 2014;15(12):550.

Fig 1. Development of resistance following trickle *T. muris* infection

C57BL/6 mice were infected repeatedly with low doses of *T. muris* infection. A) Total worm burdens. B) Faecal egg counts of week 11 infected mice. C) Adult and larval *Trichuris* worm burdens, n=5. D) CD4+ T cell percentage from large intestinal lamina propria, Th1 (Tbet+), Th2 (GATA3+), Th17 (RORγt+), Tregs (FOXP3+), n=10, from two

786 independent experiments. CD4+ T cell percentage calculated as percentage of all live
787 cells. T cell subset percentage calculated as percentage of all CD4+ cells. E) Cytokine
788 production from re-stimulated MLN cells collected at 11 weeks p.i., n=5. Statistical
789 analysis completed by one way- ANOVA or unpaired t test. Data presented as mean +/-
790 SEM. *=p<0.05, **=p<0.01, ****=p< 0.0001. Representative data from 2 independent
791 experiments.
792
793 **Fig 2. Goblet cell responses in *T. muris* trickle infected mice**
794 Caecal sections from trickle infected mice were PAS stained and goblet cells and crypt
795 length were analyzed. (A) Representative imagines of PAS stained caecal sections. (B)
796 Goblet cell counts per crypt. (C) Goblet cell size measured by goblet cell diameter. (D)
797 Crypt length. (E) Representative imagines of HID-AB caecal section to visualize
798 sulphated (black) and sialylated (blue) mucins. n=5, statistical analysis completed by a
799 one way-ANOVA. Data presented as mean +/- SEM. *=p<0.05, **=p<0.01, ***=p<0.001,
800 ****=p< 0.0001.
801
802 **Fig 3: Mucin production in *T. muris* trickle infection**
803 (A) Relative expression of goblet cell secreted products measured by qPCR. (B) Western
804 blot to visualize Muc5ac protein from extracted mucus from naïve or *T. muris* infected
805 C57Bl/6 mice at 11 weeks p.i.. (C) Muc2+ goblet cells per crypt and representative
806 immunostained sections during trickle infection. Muc2 in green. DAPI stain in blue. n=5,
807 statistical analysis completed by a one way-ANOVA comparing each time point to week
808 0. Data presented as mean +/- SEM, *=p<0.05.

Fig 4. Epithelial cell turn over following *T. muris* trickle infection

Mice were I.P. injected with BrdU to identify proliferating cells. (A) Caecal sections were stained for anti-BrdU (green) and DAPI (blue) and the distance the furthest BrdU stained cell was measured. (B) Quantification of epithelial turnover measured by BrdU incorporation into proliferating cells. (C) Relative expression of amphiregulin in the caecum measured by qPCR. n=5, statistical analysis completed by a one way-ANOVA or unpaired t test. Data presented as mean +/- SEM, **=p<0.01.

Fig 5. Challenge infection of *T. muris* trickled mice

To determine whether trickle infection could protect against a challenge infection, trickle infected mice were either left to expel all worms naturally or were removed by anti-helminthic treatment. (A) At week 30, when no worms were present, determined by measuring faecal egg output, mice were challenged with a single low dose infection. Control mice of a single low dose, single high dose or no primary infection were also challenged at week 30 post infection n = 10 or greater. (B) Following trickle infection mice were treated with anti-helminthic to remove final worms at week 11 post infection. Naïve mice and trickled mice were challenged with a low dose infection one week after anti-helminthic treatment. n=5 representative of two independent experiments, statistical analysis completed by a one way ANOVA or an unpaired t test. Data presented as mean +/- SEM, *=p<0.05, **=p<0.01, ***=p<0.001, ****=p< 0.0001.

Fig 6. CD4+ depletion in *T. muris* trickle infection

(A) Worm burdens of *T. muris* trickle infected Rag-/- (black) and C57Bl/6 (grey) mice, n=5. Adult worms and larval stages 4-2 were counted. Mice were treated with 200µg anti-CD4 antibody or isotype control antibody, 3 times a week for 3 weeks (weeks 8-10 of trickle infection). (B) FACS analysis of CD4+ T cells to confirm depletion. (C) Total worm burdens of *T. muris* infected mice at week 11. (D) Adult worms and larval stage counts following CD4+ depletion at week 11 trickle infection, n=9-10, based on two experiments. Statistical analysis completed using an unpaired t test. Data presented as mean +/- SEM, *=p<0.05, **=p<0.01, ***=p<0.001, ****=p< 0.0001.

Fig 7. Changes in worm expulsion mechanisms following CD4+ T cell depletion in trickle infection.

Following CD4+ T cell depletion worm expulsion mechanism were analyzed. (A) Representative images of PAS stained caecal sections to measure crypt length and goblet cell counts per crypt, n=5. (B) Relative expression of Muc5ac and RELM-beta analyzed by qPCR, n=5. (C) Epithelial cell turn over measured by furthest distanced BrdU stained cells travelled up intestinal crypt. Sections stained by anti-BrdU (green) and DAPI (blue), n=4-5. Statistics measured using an unpaired t test. Data presented as mean +/- SEM, *=p<0.05, **=p<0.01.

Fig 8. Innate lymphoid cells and tuft cell proliferation in *T.muris* trickle infection.

(A) Innate lymphoid cell percentage measured by FACS, identified as lineage negative, CD90.2+, CD127+. (B) Tuft cells in caecal and small intestine sections of trickle infected

mice. Tuft cells identified as DclK1 positive cells in green. DAPI stain in blue. n=5, statistical analysis completed by a one way-ANOVA, *=p<0.05.

Fig 9. Depletion of ILC2s in ICOS-T mice during *T. muris* trickle infection.

ILC2s were depleted from ICOS-T mice by DTx treatment. (A) Mice received 750ng DTx (red arrow) for 10 days at week 8-10 of trickle infection (purple arrow) where mice were infected weekly for 9 weeks with 20 eggs. Control mice received PBS control injections at the same time points. Two weeks following the final trickle infection worm burdens and ILC2 depletion was analyzed. (B) Flow cytometry to confirm depletion, ILC2s identified as Lineage-, CD127+, CD90.2+, GATA3+ cells. ILC2% of all ILCs and ILC2 counts. (C) Total worm burdens of trickle infected mice. (D) Worm burdens of developmental stages during trickle infection. Statistical analysis completed by an unpaired t-test. Data presented as mean +/- SEM, *=p<0.05. n=6-7 representative of two experiments.

Fig 10. NMDS analysis of fecal microbial communities during low dose and trickle *T. muris* infection.

(A) NMDS plot of microbial communities during *T. muris* Low Dose infection. Naïve mice (blue) were compared to mice trickled with *T. muris* (purple) at 9 and 11 weeks post infection (◯ & □). Infection and time drove significant changes in microbiome composition ($p = 0.001$ & $p = 0.05$) assessed by PERMANOVA. (B) NMDS plot of microbial communities during *T. muris* trickle infection. Naïve mice (blue) were compared to mice trickled with *T. muris* (red) at 9 and 11 weeks post infection (◯ & □). Infection drove a

876 significant change in microbiome composition ($p < 0.004$) assessed by PERMANOVA.
877 Axes represent a scale of Euclidian distances between samples where the centre is zero.
878 Stress measures quality of fit (< 0.1 indicates a very good fit). (C & D) Alpha diversity of
879 (C) low dose and (D) trickle infected mice given calculated in R by Shannon diversity test
880 using the Vegan package. Significance is calculated by two-way ANOVA. Data presented
881 as mean, * = $p<0.05$, ** = $p<0.01$, **** = $p<0.0001$.
882
883 **Fig 11. Comparative abundance of bacterial genera in naïve and trickled mice.**
884 Bubble plot representing the relative abundance of the top 20 genera determined as those
885 with the highest median abundance across all individuals (as a proportion of total
886 microbial composition). Circle size is representative of the proportion of the microbiota
887 comprised by that genus. Empty spaces indicate that there was no detection of that genus
888 by 16S sequencing.
889
890 **Supplementary Fig 1. *T. muris* trickle infection regime.**
891 C57BL/6 mice were infected weekly with low doses of *T. muris* (20 eggs) for 3, 5, 7 or 9
892 weeks (red arrow). 2 weeks after the final infectious dose at week 5, 7, 9 and 11, worm
893 burdens and immune responses were analysed (black box).
894
895 **Supplementary Fig 2. CD4+ T cells in MLN following *T. muris* trickle infection.**
896 C57BL/6 mice were infected weekly with low doses of *T. muris* and 2 weeks after the
897 final trickle infection CD4+ T cells were analyzed by FACs. CD4+ Th1 (Tbet+), Th2
898 (GATA3+), Th17 (RORγt+), Tregs (FOXP3+), n=10, from two independent experiments.

CD4+ T cell percentage calculated as percentage of all live cells. T cell subset percentage calculated as percentage of all CD4+ cells.

Supplementary Fig 3. *T. muris* specific antibody responses in trickle infected mice. Antibody responses measured from sera collected from trickle infected mice, measured by an ELISA. The antibody response specific for adult worms and larval stages 1-4 was measured. (A) IgG1 response. (B) IgG2a/c response. (C) Total IgE response. n=5, statistical analysis completed by a one way-ANOVA. Data presented as mean +/- SEM, *=p<0.05, **=p<0.01, ****=p< 0.0001.

Supplementary Fig 4. *T. muris* specific antibody responses following CD4+ T cell depletion.

Sera from *T. muris* infected mice depleted of CD4+ T cells was collected and IgG1 and IgG2a responses specific for *T. muris* larval stages was measured by an ELISA. A) IgG1 response to adult worms and larval stages 1-4. B) IgG2a response to adult worms and larval stages 1-4. Isotype control in grey. Anti-CD4 treatment mice in black. n=5

Supplementary Fig 5. ILCs counts in MLN.

Innate lymphoid cell counts and percentage in the MLN following *T. muris* trickle infection measured by FACS, identified as lineage negative, CD90.2+, CD127+. Total ILC percentage calculated as percentage of all live cells. ILC subset calculated as the percentage of total ILCs. n=3, statistical analysis completed by a one way-ANOVA. Data presented as mean +/- SEM, *=p<0.05, **=p<0.01

Supplementary Fig 6. Depletion of ILC2s in ICOS-T mice.

ILC2s were depleted from ICOS-T mice by DTx treatment. (A) Mice received 750ng DTx (red arrow) for 5 days before *T. muris* high dose (400 eggs) infection (purple arrow) and 1 week after *T. muris* infection for 5 days. Control mice received PBS control injections at the same time points. Worm burden was analysed at week 5 p.i. (black arrow) (B) Flow cytometry to confirm depletion, ILC2s identified as Lineage-, CD127+, CD90.2+, GATA3+ cells. ILC2% of all ILCs and ILC2 counts. (C) Worm burden of *T. muris* at day 35 p.i. Statistical analysis completed by an unpaired t-test. . Data presented as mean +/- SEM, *=p<0.05. n=3-5.

Supplementary Fig 7. Immediate hypersensitivity response to OVA antigen during *Trichuris muris* infection.

C57BL/6 mice were infected with a single low dose or trickled with *T. muris* over 9 weeks. At week 8 following the first infection mice were sensitized with 50 µg OVA antigen in 2mg of Alum or PBS control for 3 weeks. 4 weeks following the final sensitization all mice were challenged with 50 µg OVA by intradermal injection in the right ear and a PBS control injection in the left ear. A) Timeline of *T. muris* infection and sensitisation and challenge of OVA/PBS. B) Immediate hypersensitivity response in mice following PBS and OVA challenge. C) Immediate hypersensitivity in *T. muris* infected mice sensitised with OVA antigen. D) Worm burdens of *T. muris* trickle infected mice. Data presented as mean +/-

SEM. Statistical test calculated by an unpaired t-test, **=p<0.01, ***=p<0.001, ****=p< 0.0001, n=5.

Supplementary Fig 8. Co-infection of *Trichuris muris* with *Nippostrongylus brasiliensis*.

C57BL/6 mice were infected with a single *T. muris* low dose (20 eggs) or trickle infected of 9 weekly low doses by oral gavage. At week 10, *T. muris* infected mice and naive mice were infected with a single high dose (300 larvae) of *N. brasiliensis* by subcutaneous injection. At day 3 and day 6 following the *N. brasiliensis* infection, worm burdens of *N. brasiliensis* from the lung and small intestine and *T. muris* in the caecum, were counted. A) Timeline of infection regime. B) Worm burdens of *N. brasiliensis* in the small intestine and lung. C) *T. muris* worm burdens from low dose infected and trickle infected mice. Burdens of total worms and well as adult, L4, L3 and L2 were counted for trickle infected mice. Data presented as mean +/- SEM. Statistical analysis was carried out using a one-way ANOVA followed by post-hoc Tukey's test. n=5.

Supplementary Fig 9. Composition of microbial communities during infection.

(A) Rarefaction curves for individual samples calculated in R using the vegan package. (B) Phylum level comparisons between samples. Phyla representing, on average, less than 2% of the population were grouped into "other."

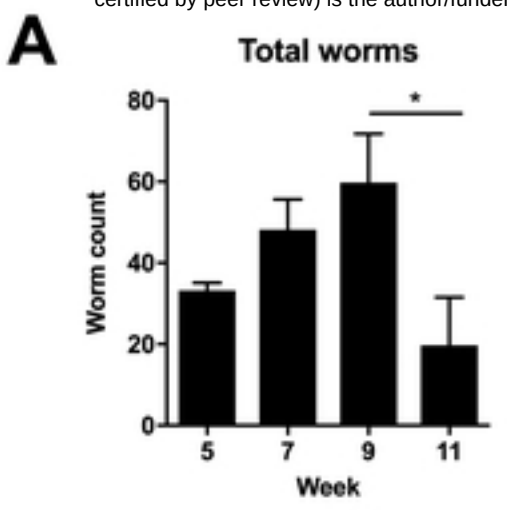

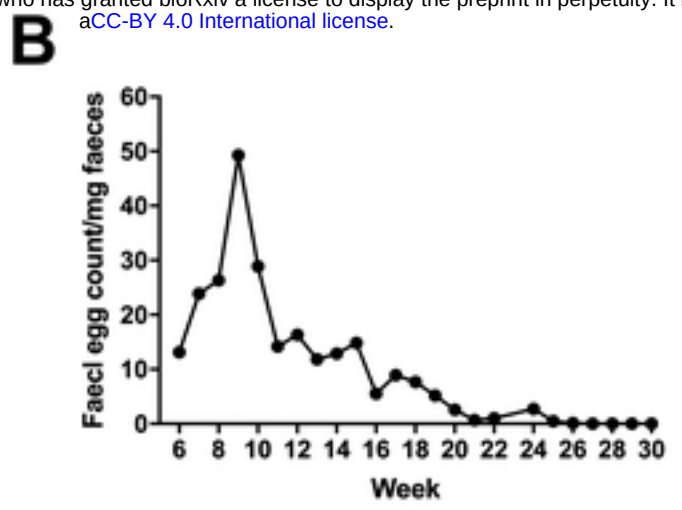

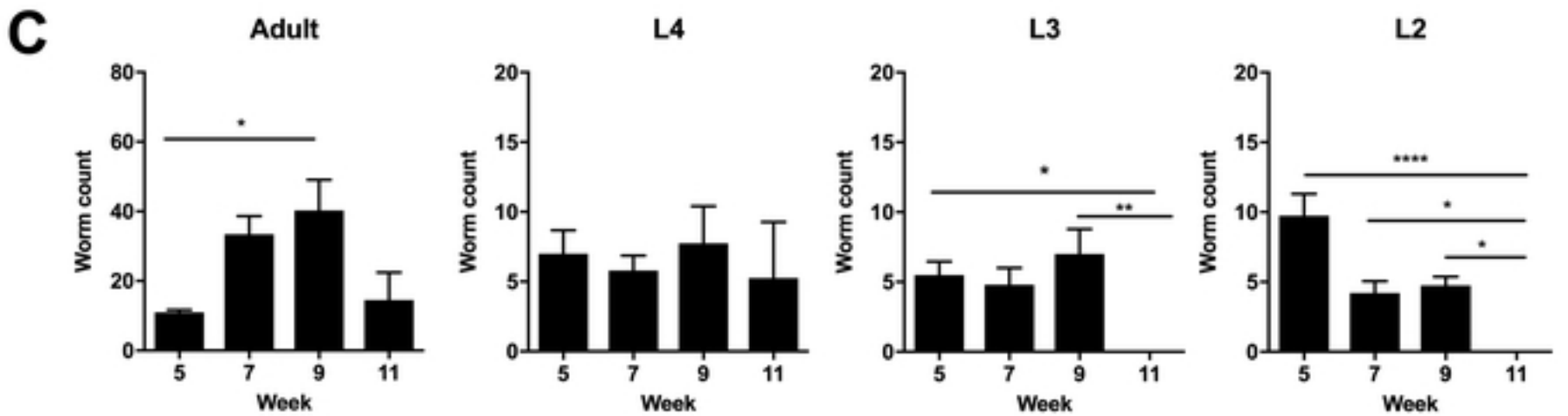

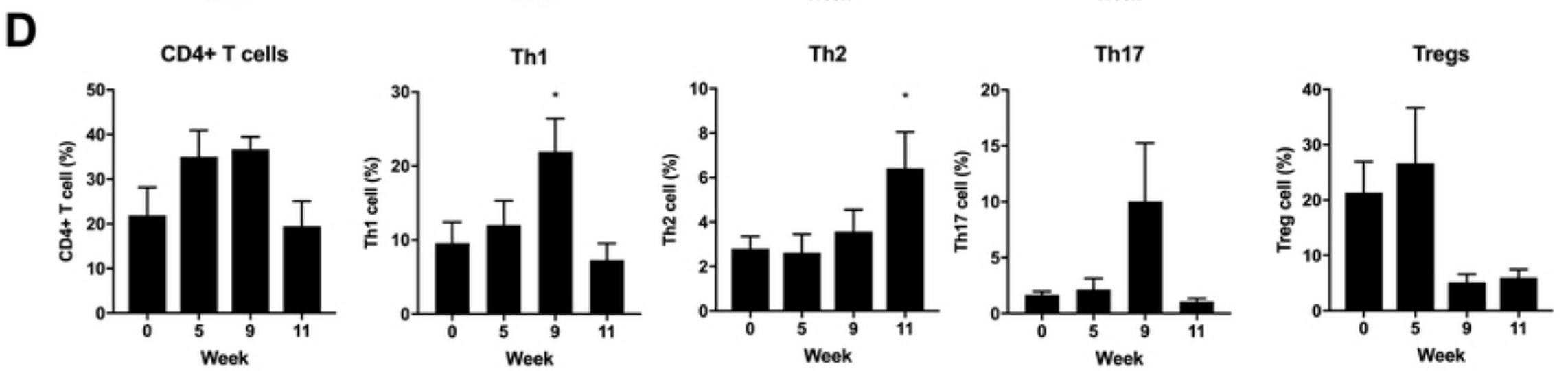

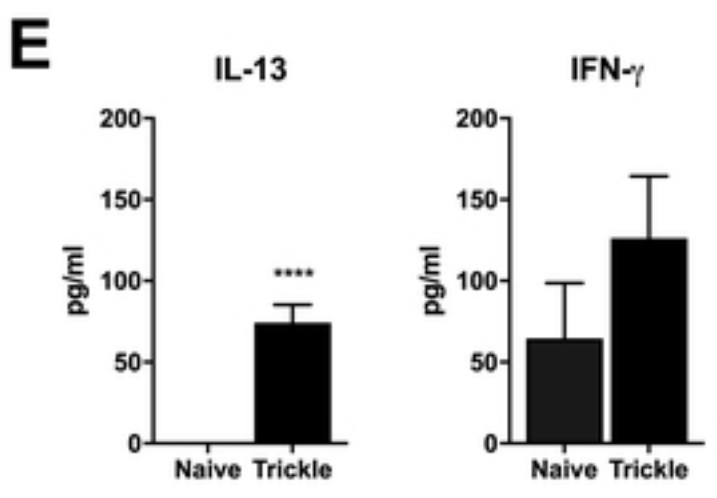

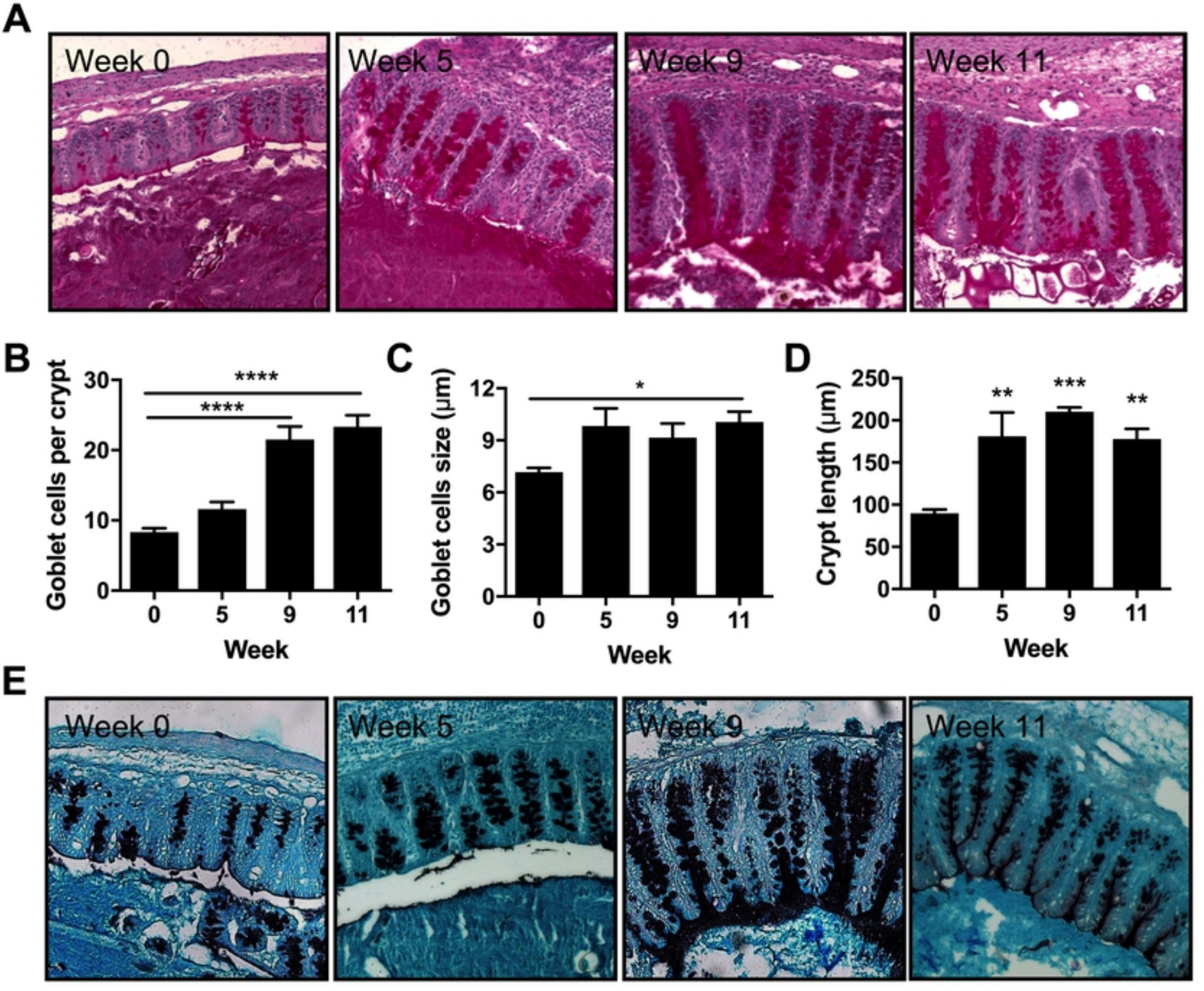
A
Week 0
Week 5
Week 9
Week 11
B
Goblet cells per crypt
30
20
10
0
****
****
0
5
9
11
Week
C
Goblet cells size (µm)
12
9
6
3
0
*
0
5
9
11
Week
D
Crypt length (µm)
250
200
150
100
50
0
**
***
**
0
5
9
11
Week
E
Week 0
Week 5
Week 9
Week 11

A

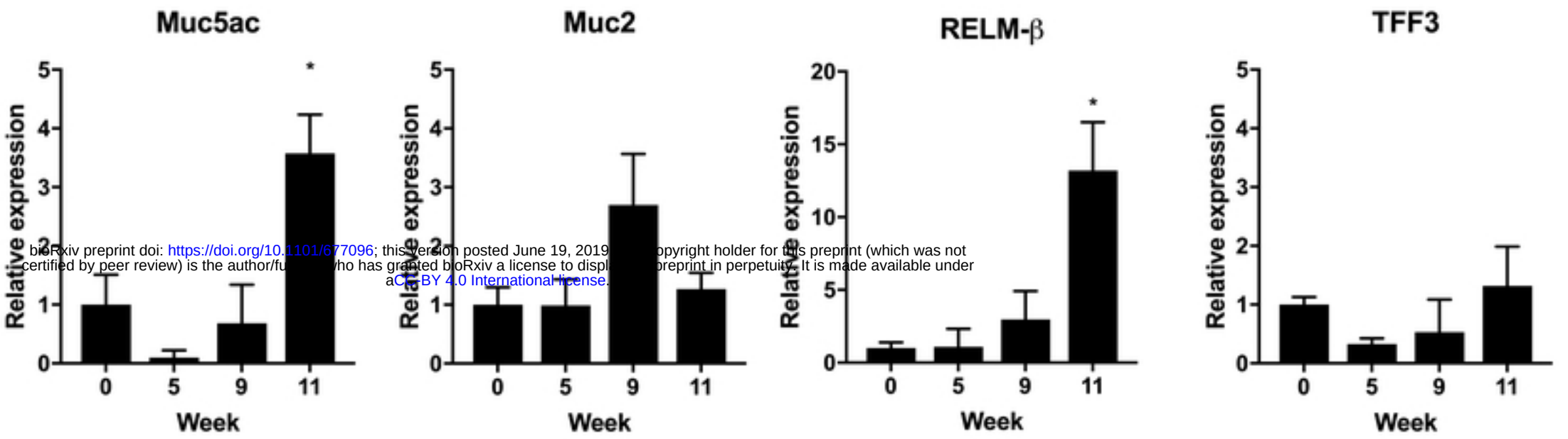

B

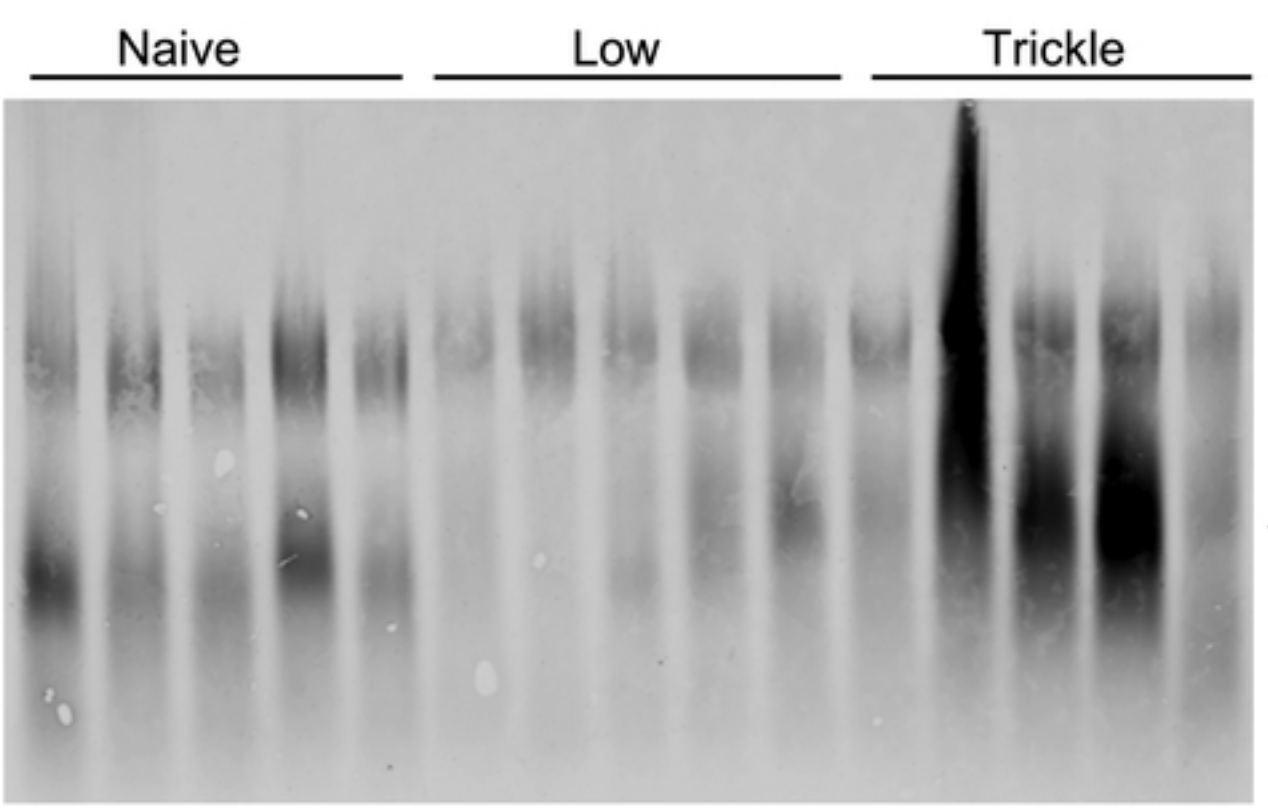

C

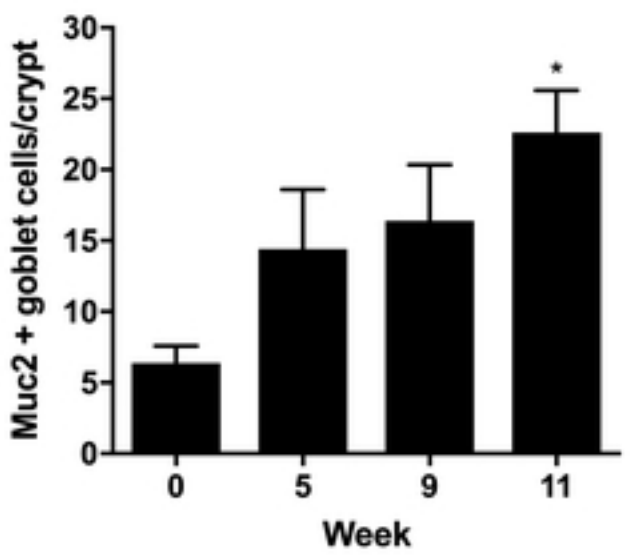

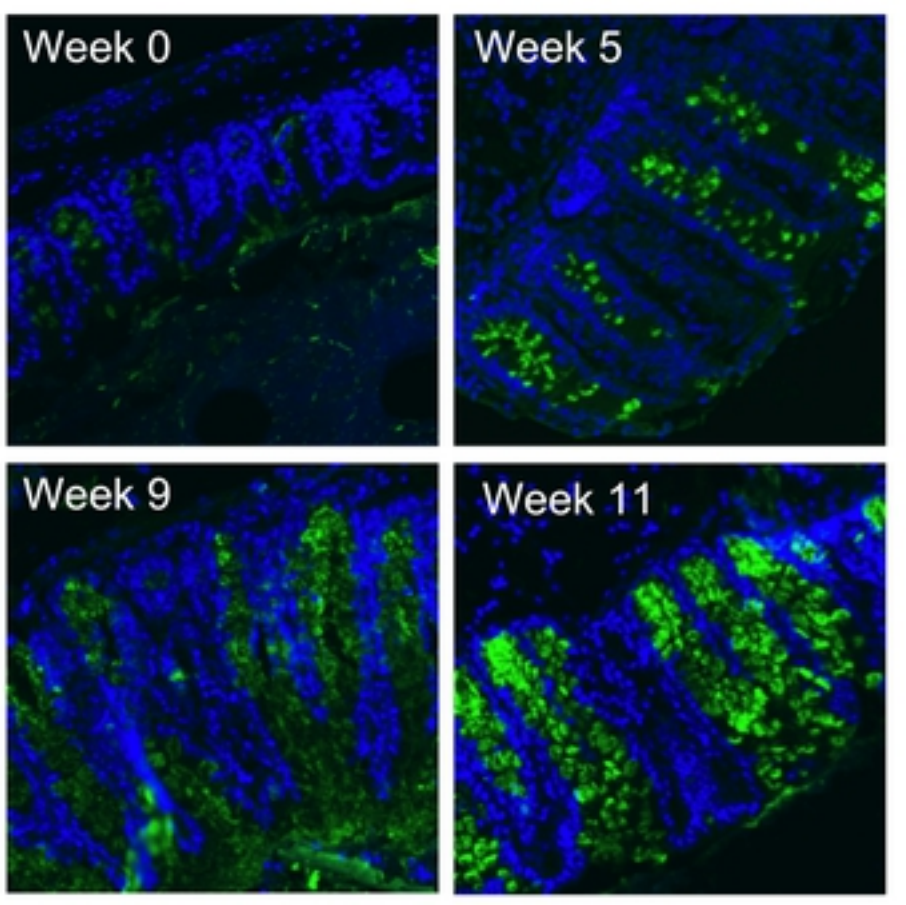

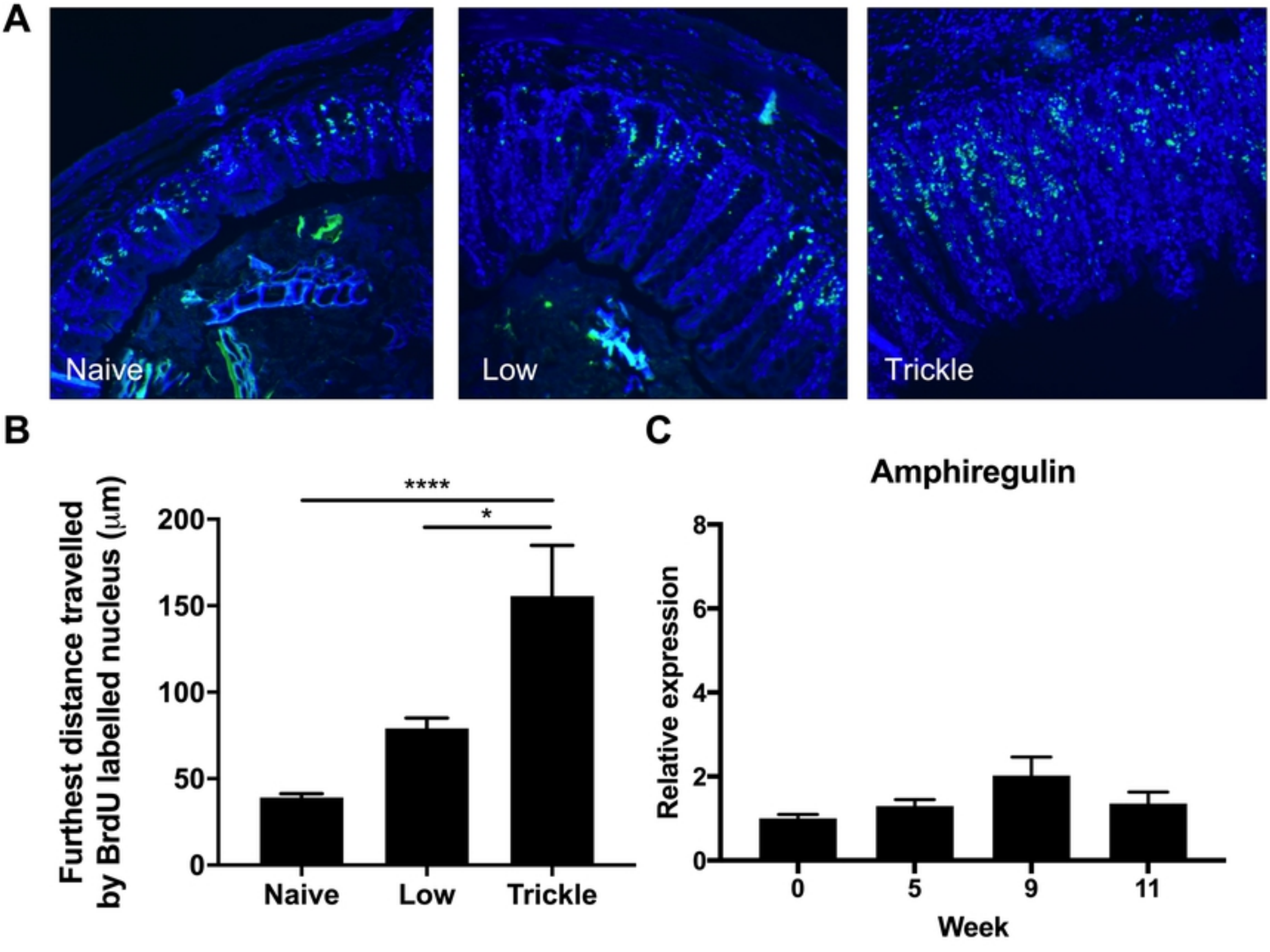
A
Naive
Low
Trickle
B
Furthest distance travelled by BrdU labelled nucleus (μm)
****
*
200
150
100
50
0
Naive
Low
Trickle
C
Amphiregulin
Relative expression
8
6
4
2
0
0
5
9
11
Week

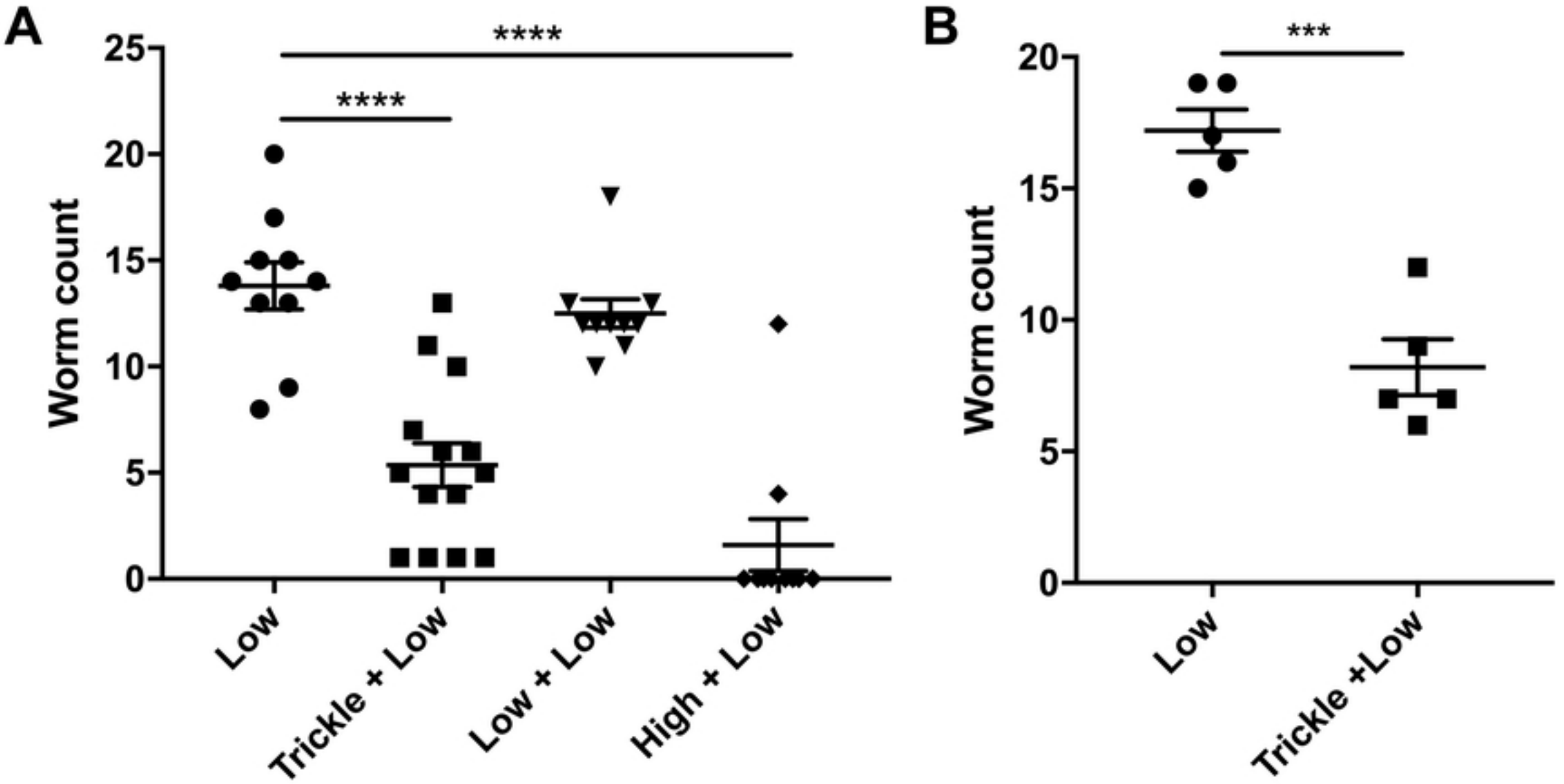
A
****
****
Worm count
25
20
15
10
5
0
Low
Trickle + Low
Low + Low
High + Low
B
***
Worm count
20
15
10
5
0
Low
Trickle +Low

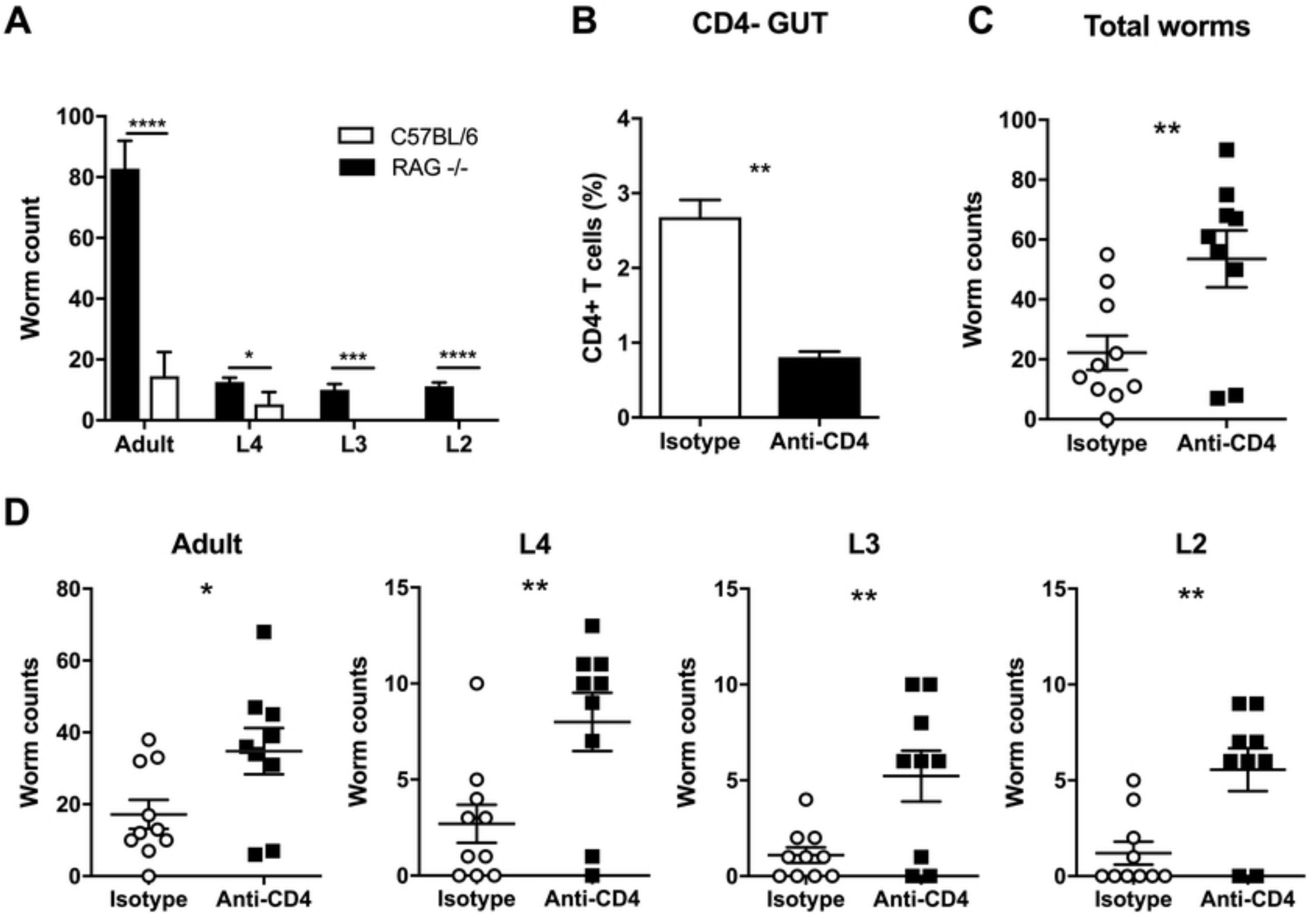
A
Worm count
C57BL/6
RAG -/-
****
*
***
****
Adult
L4
L3
L2
B
CD4- GUT
CD4+ T cells (%)
**
Isotype
Anti-CD4
C
Total worms
Worm counts
**
Isotype
Anti-CD4
D
Adult
*
L4
**
L3
**
L2
**
Worm counts
Isotype
Anti-CD4

A

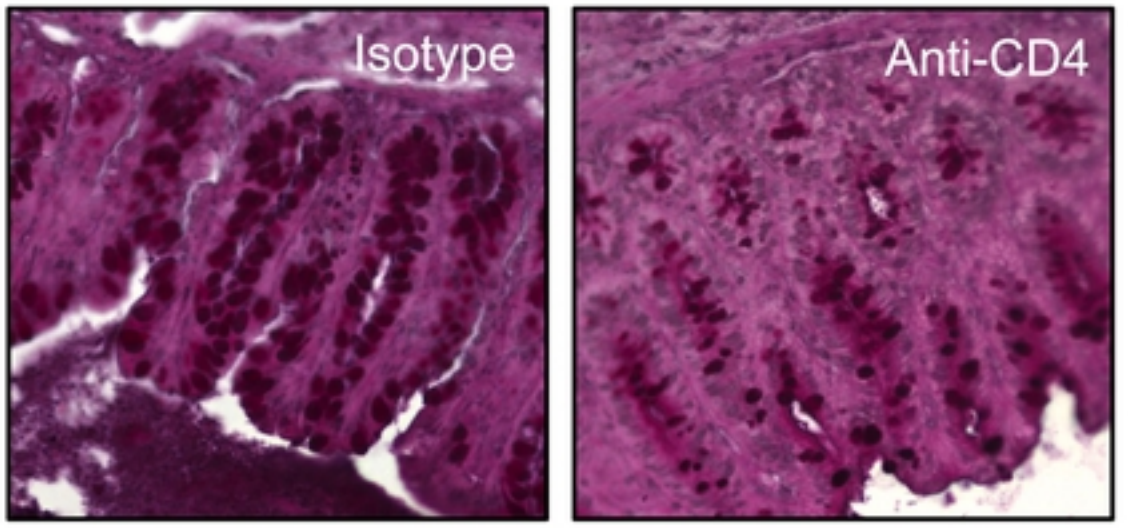
Isotype
Anti-CD4

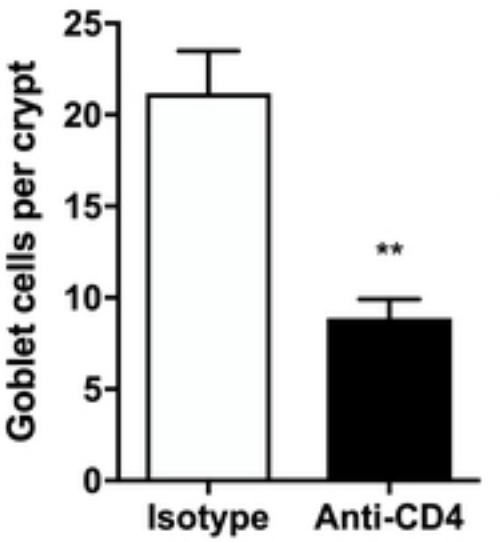
Goblet cells per crypt
25
20
15
10
5
0
**
Isotype
Anti-CD4

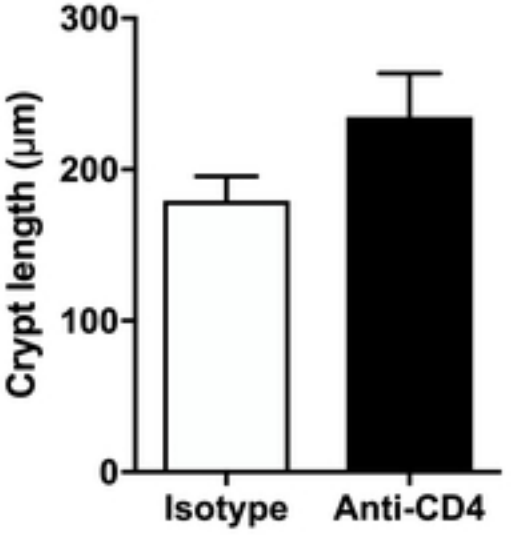
Crypt length (μm)
300
200
100
0
Isotype
Anti-CD4

B

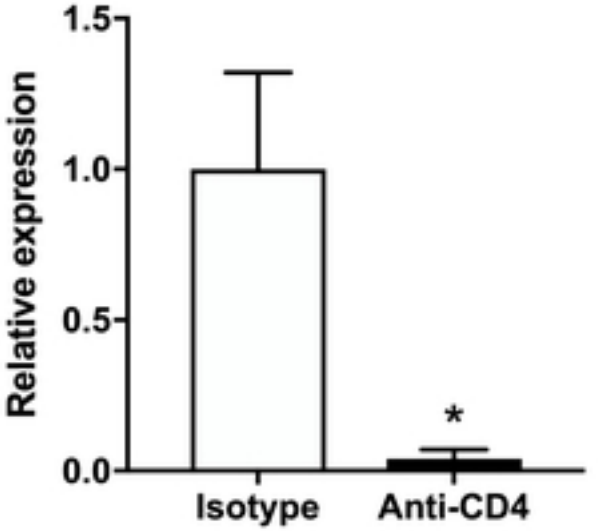
Muc5ac
Relative expression
1.5
1.0
0.5
0.0
*
Isotype
Anti-CD4

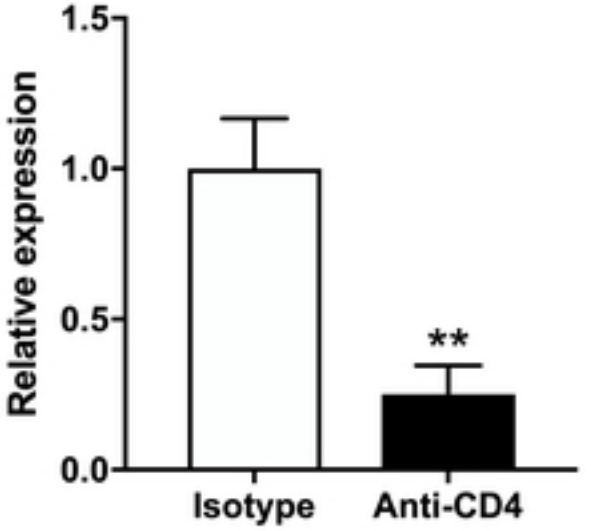
RELM-β
Relative expression
1.5
1.0
0.5
0.0
**
Isotype
Anti-CD4

C

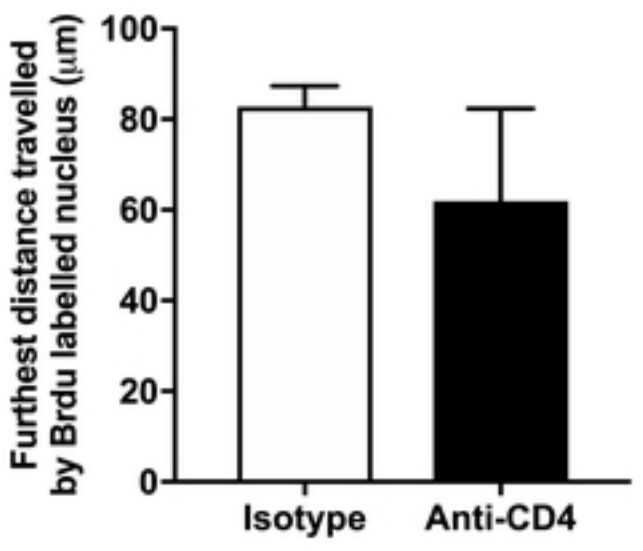
Furthest distance travelled by Brdu labelled nucleus (μm)
100
80
60
40
20
0
Isotype
Anti-CD4

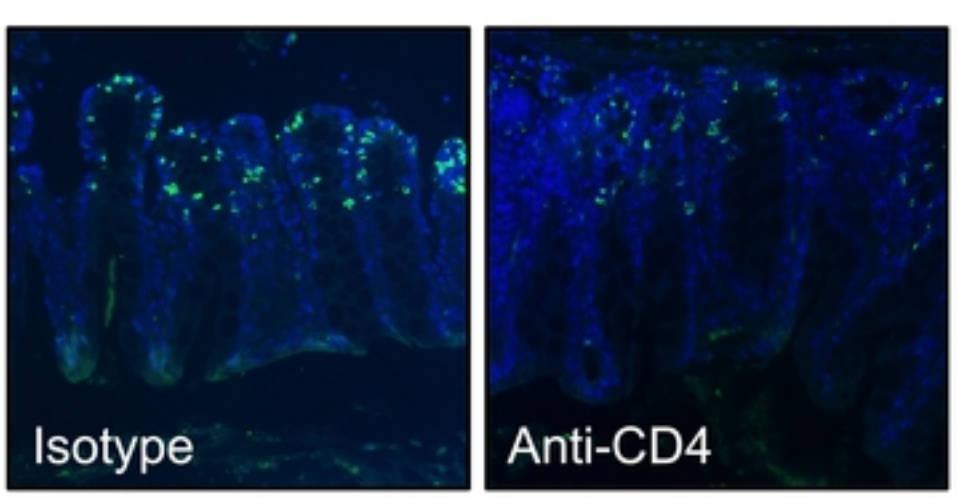
Isotype
Anti-CD4

A

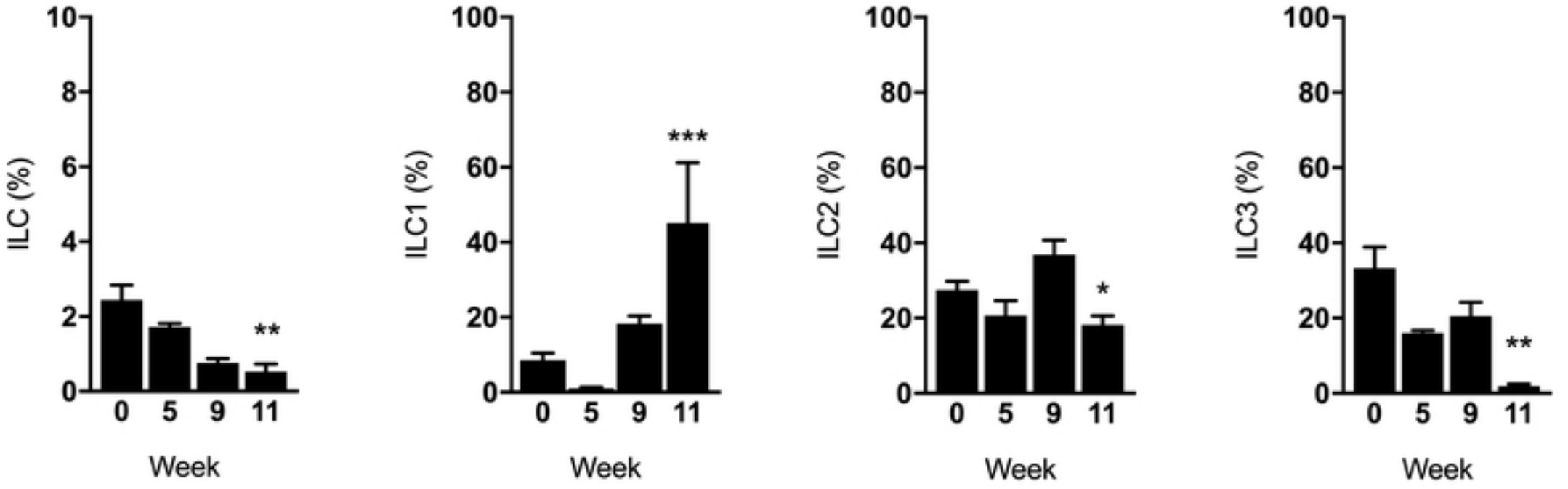

B

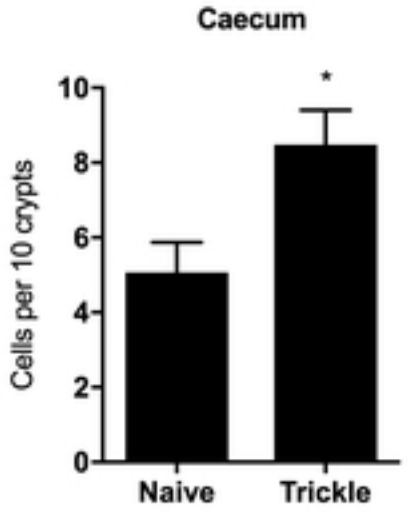

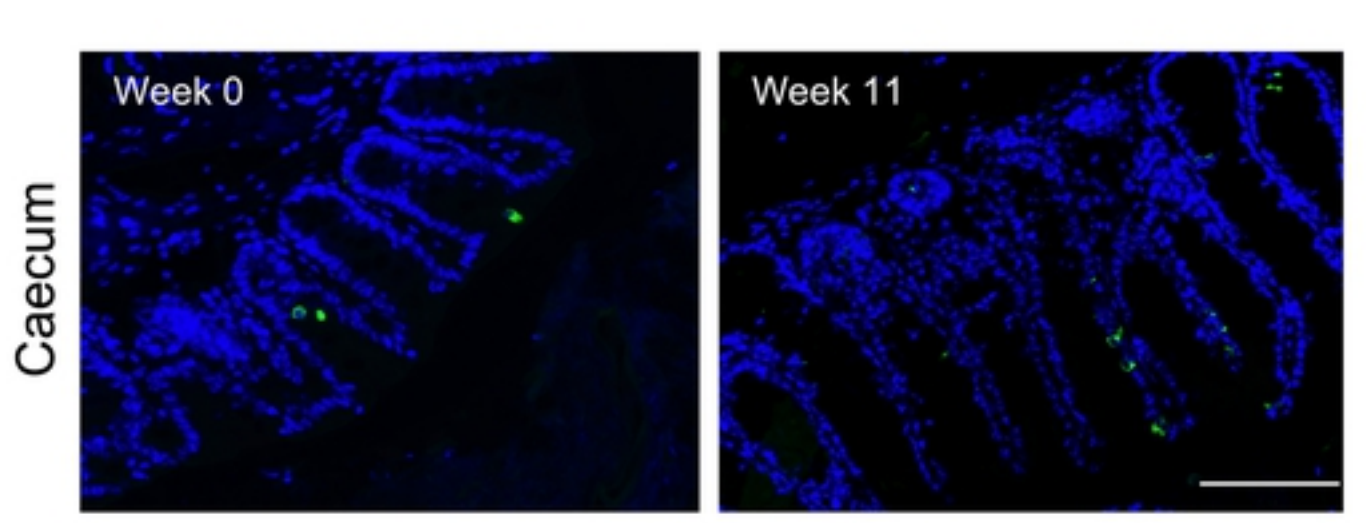

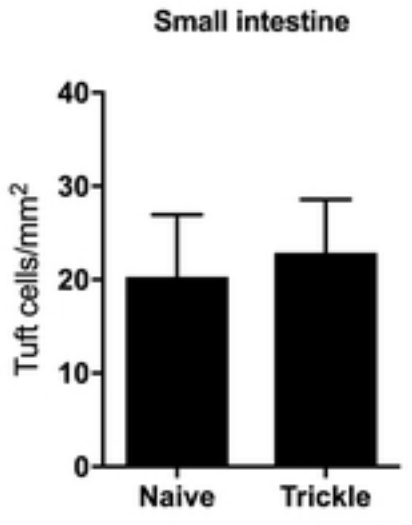

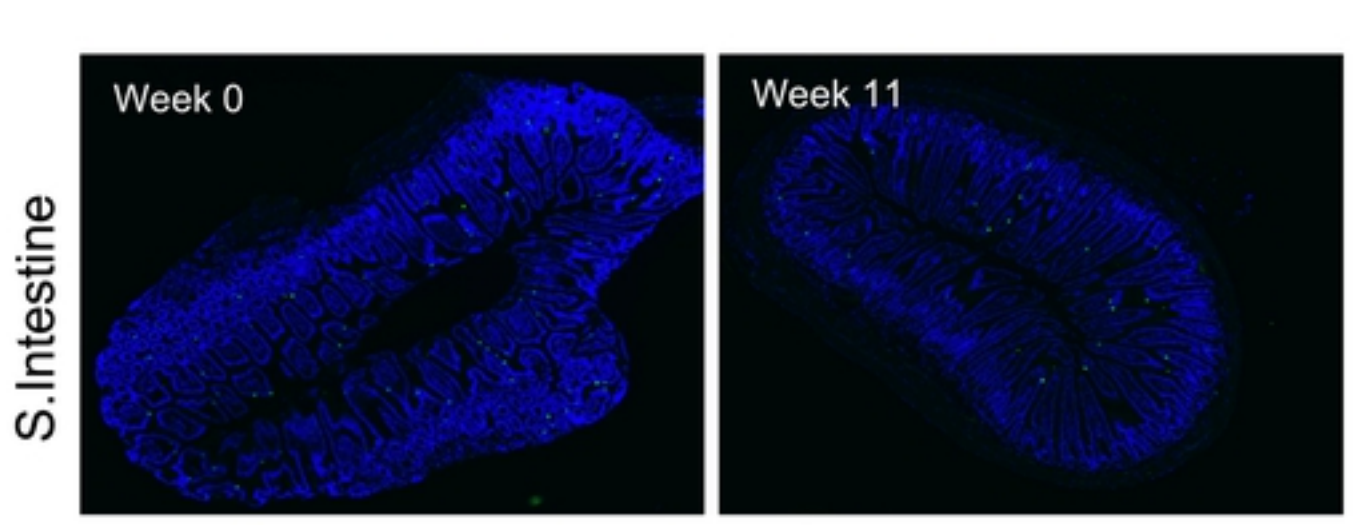

A

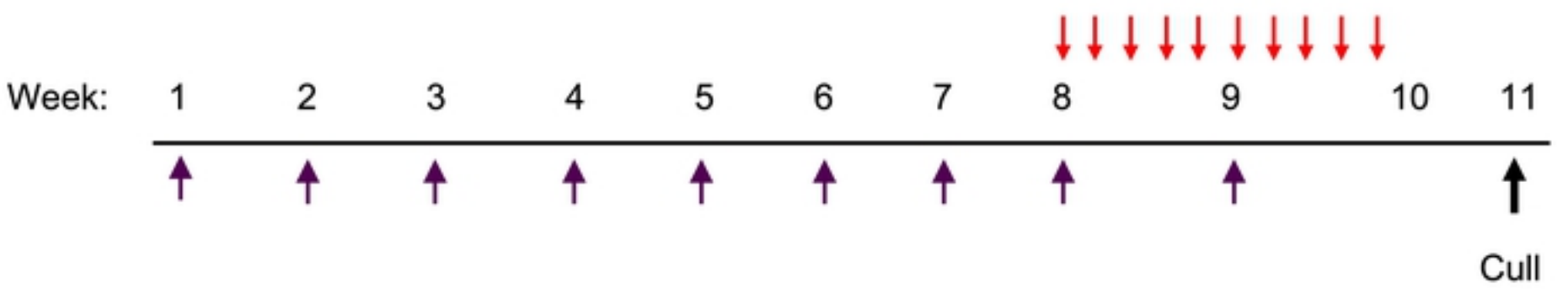
Week:
1
2
3
4
5
6
7
8
9
10
11
Cull

B

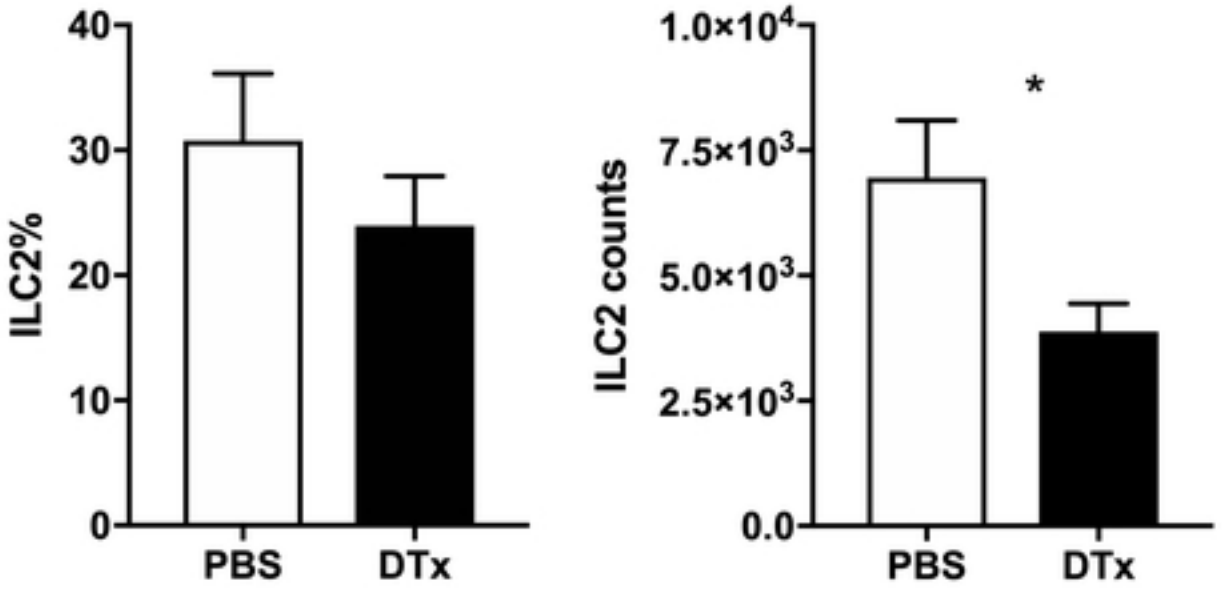
ILC2%
40
30
20
10
0
PBS
DTx
ILC2 counts
1.0×10^4
7.5×10^3
5.0×10^3
2.5×10^3
0.0
*
PBS
DTx

C

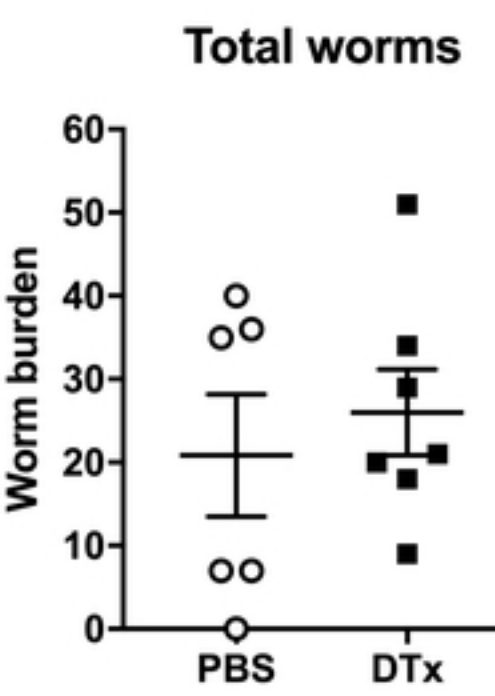
Total worms
Worm burden
60
50
40
30
20
10
0
PBS
DTx

D

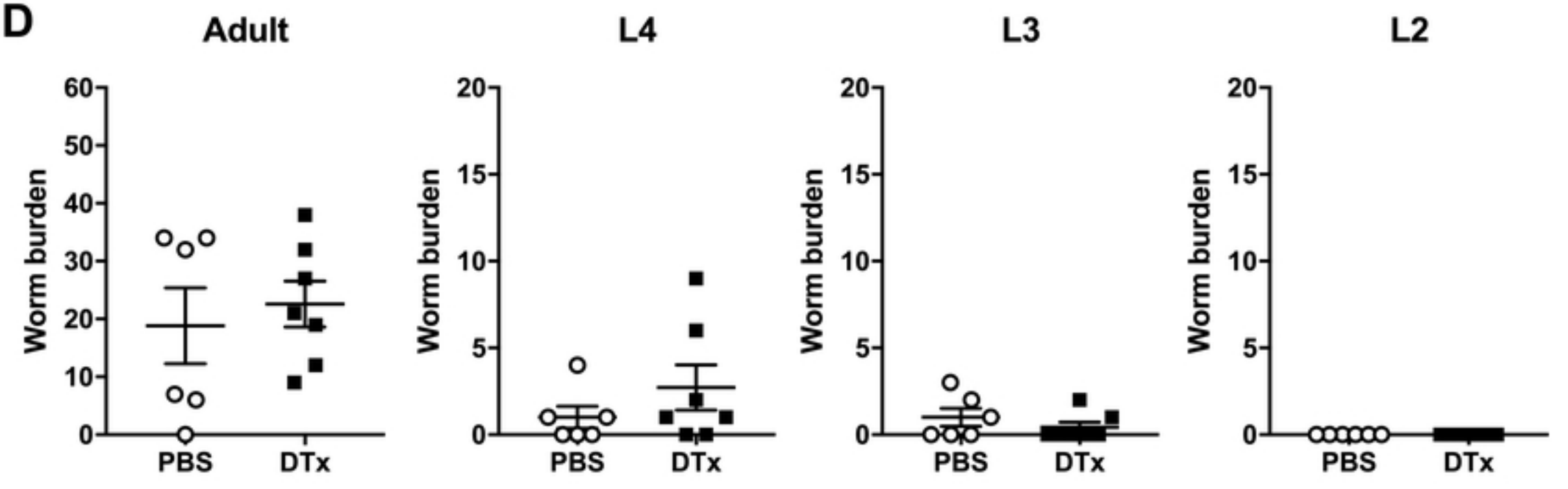
Adult
L4
L3
L2
Worm burden
PBS
DTx

A

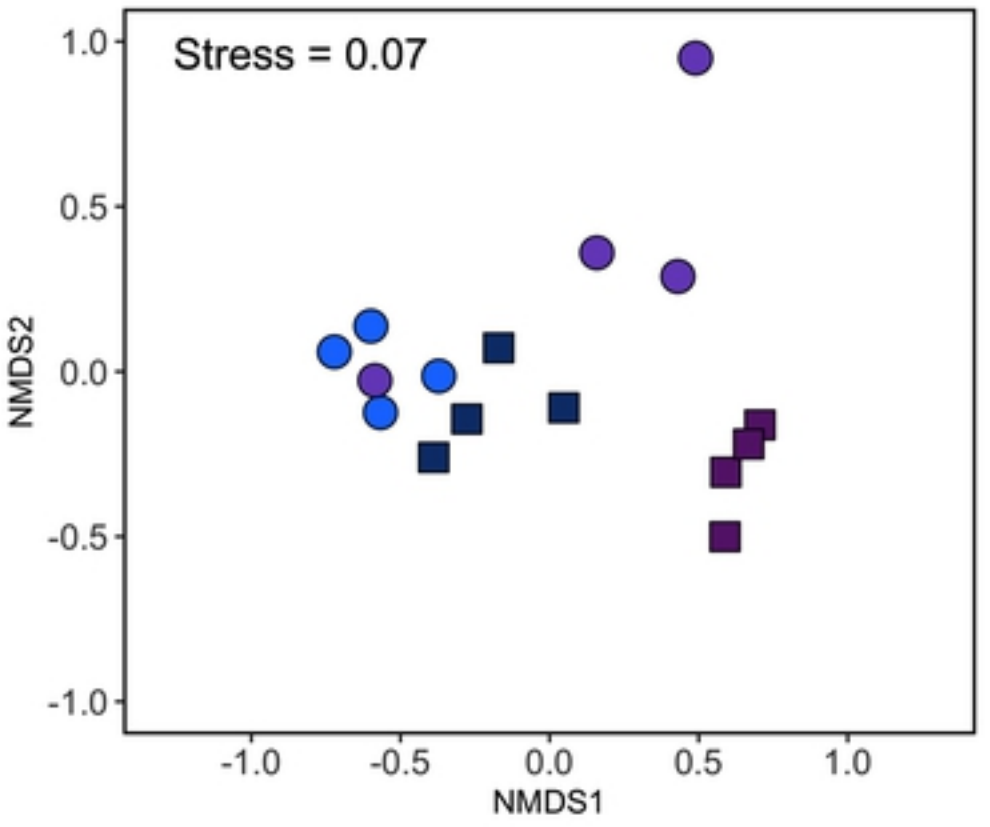

0.004

Naive Low Dose

B

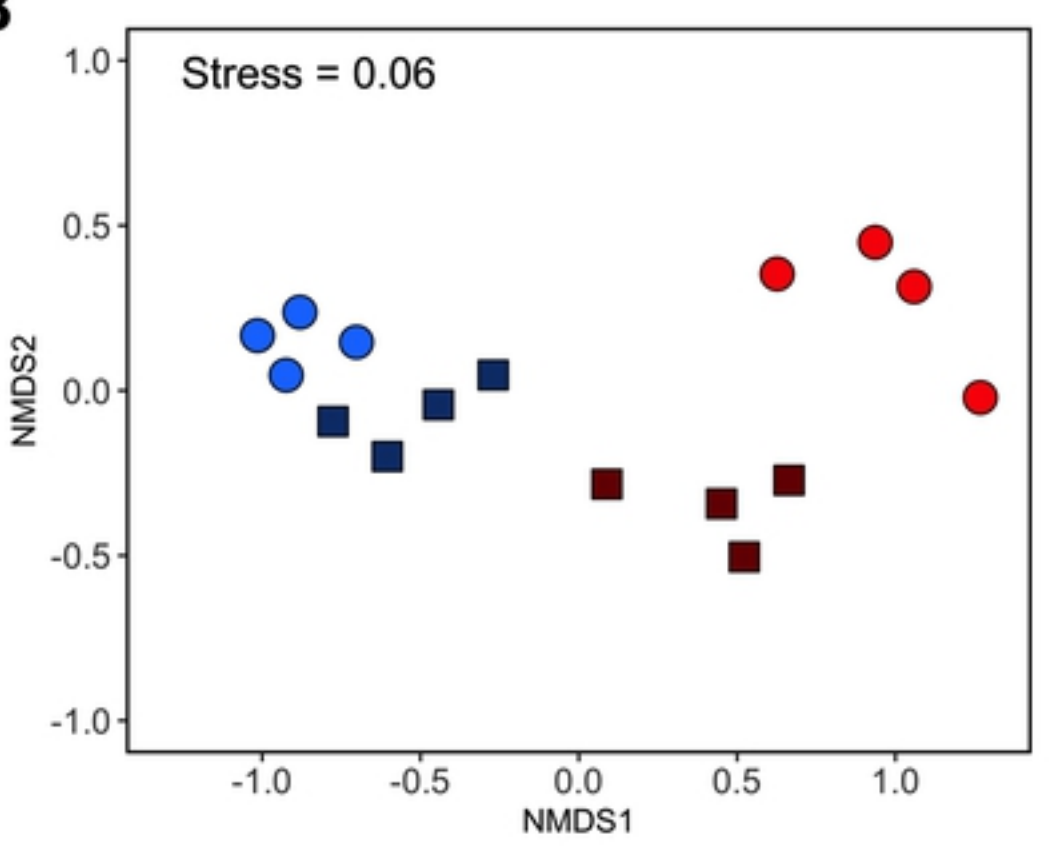

0.001

Naive Trickle

0.018

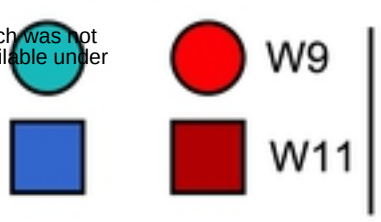

0.05

C

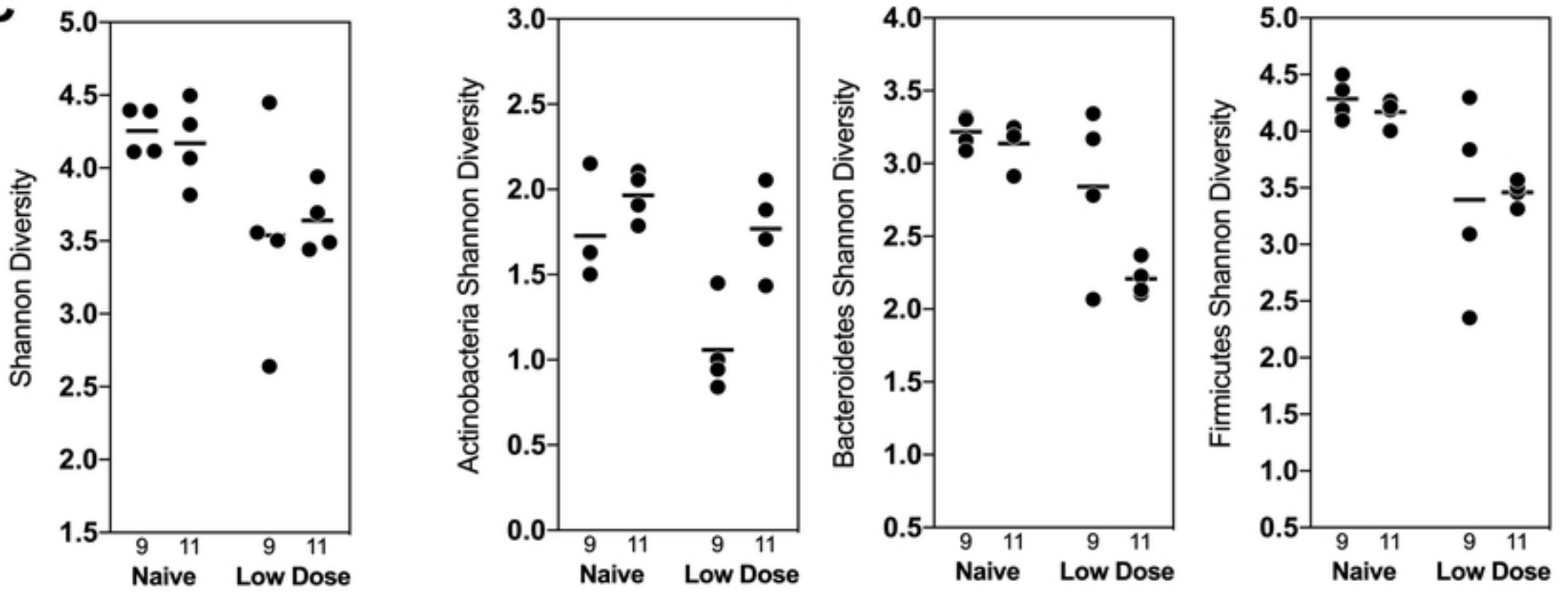

D

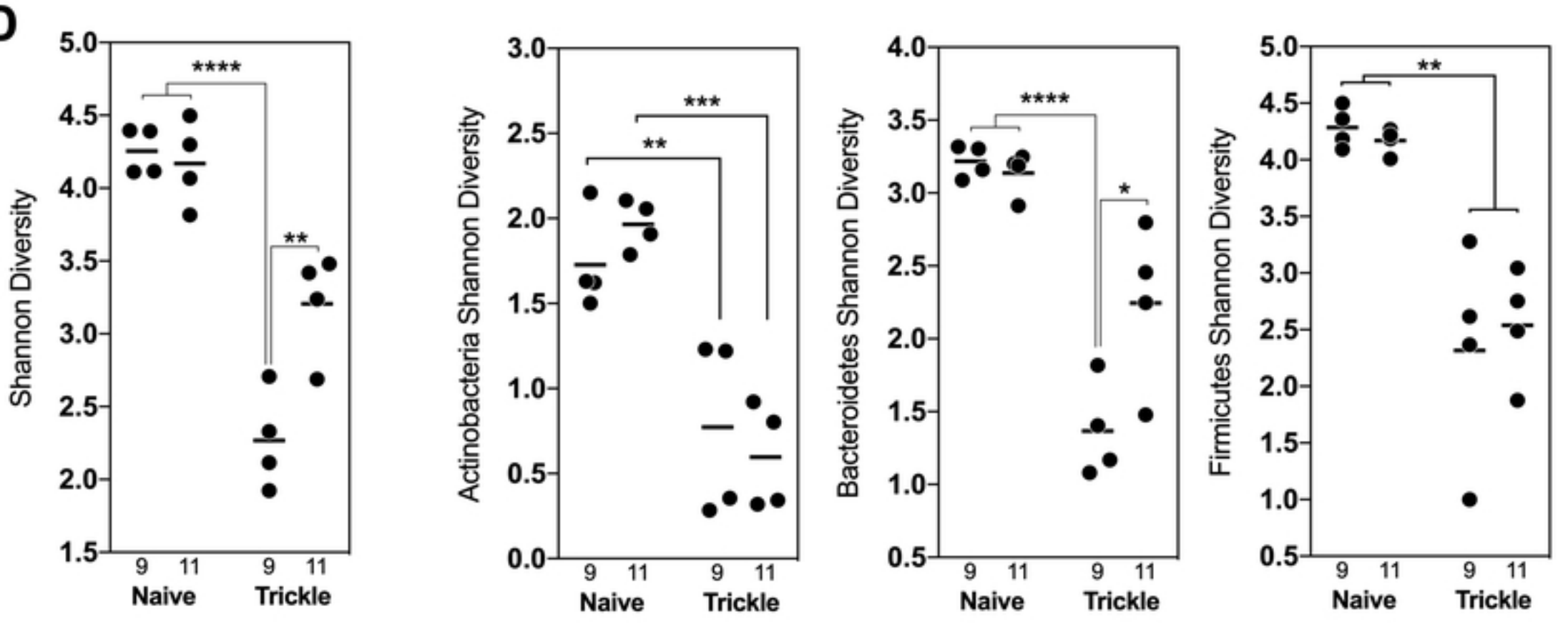

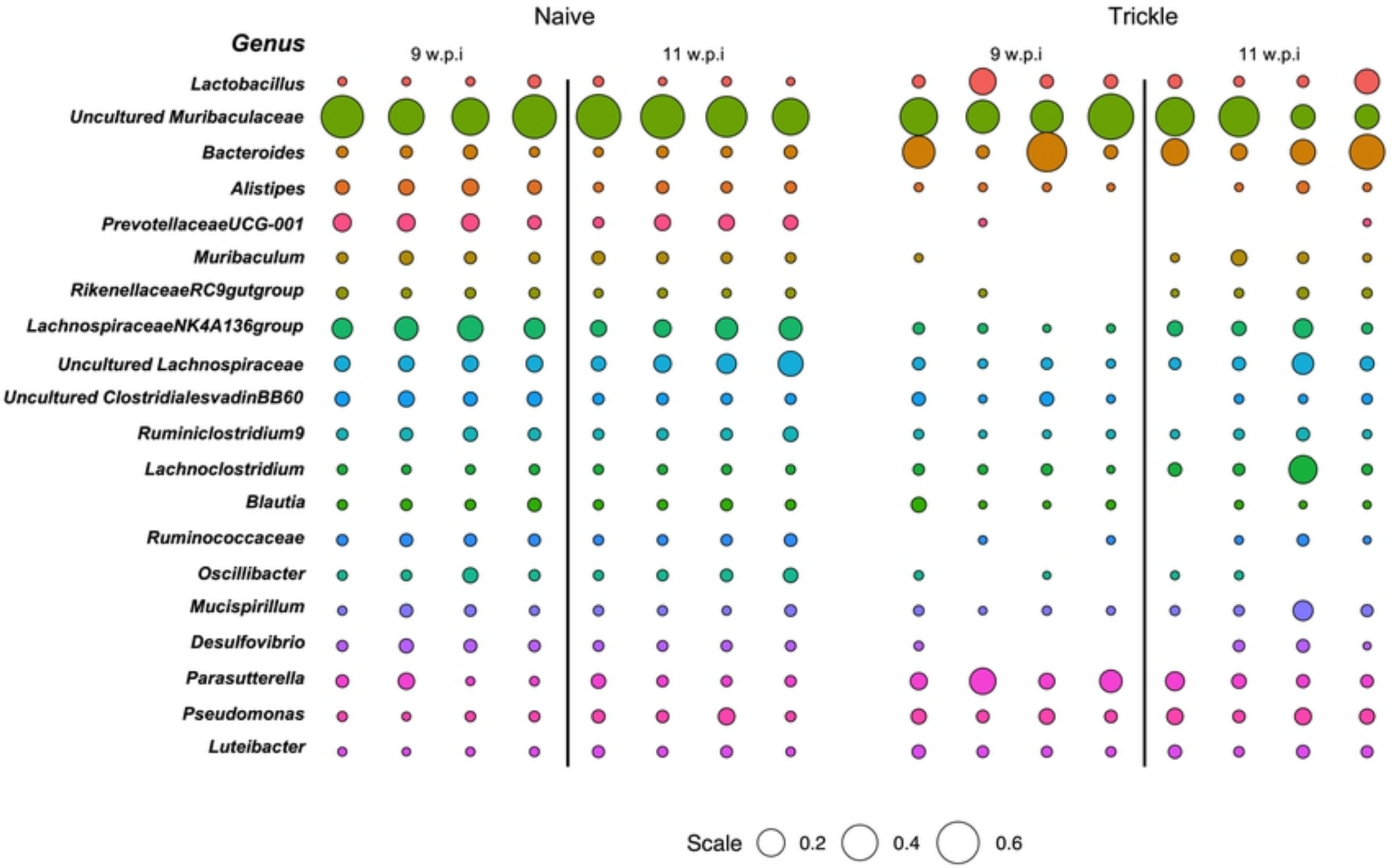
Naive
Trickle
Genus
9 w.p.i
11 w.p.i
9 w.p.i
11 w.p.i
Lactobacillus
Uncultured Muribaculaceae
Bacteroides
Alistipes
PrevotellaceaeUCG-001
Muribaculum
RikenellaceaeRC9gutgroup
LachnospiraceaeNK4A136group
Uncultured Lachnospiraceae
Uncultured ClostridialesvadinBB60
Ruminiclostridium9
Lachnoclostridium
Blautia
Ruminococcaceae
Oscillibacter
Mucispirillum
Desulfovibrio
Parasutterella
Pseudomonas
Luteibacter
Scale
0.2
0.4
0.6